Solving Environment Economic Power Dispatch Problems by Multi-objective Modified Seagull Optimization Algorithm with Novel Constraint Treatments

Gonggui Chen, Tao Tan, Wei Xiang, Zhenqi Guan, Hao Tan, Jianbo Yu, Hongyu Long*

***Abstract*—In this paper, a multi-objective modified seagull optimization algorithm (MOMSOA) is proposed to handle multi-objective environmental economic power dispatch (EED) problems. The algorithm utilizes logistic map to randomize the parameter *u*, which increases the diversity of the algorithm and speeds up the convergence rate. Besides, the mutation operator is combined to enlarge the range of the search and to avoid falling into the local optimum. The exploration as well as exploitation capabilities for MOSOA are balanced by non-linearizing the original linear parameter *A* through a cosine dynamic variation strategy. Furthermore, with the assistance of a unique constraint handling approach and non-inferior sorting, MOMSOA can obtain a set of uniform Pareto optimal solution (POS). In order to verify the effectiveness of MOMSOA, experiments were conducted on diverse test systems including IEEE30-Bus, IEEE57-Bus and IEEE118-Bus test systems. During the experimental process, MOSOA and MOPSO/MODE are compared with MOMSOA. Eight trials were conducted, and optimized objective functions include fuel cost, fuel cost with valve point effect, power loss and pollution emission. The results of experiments demonstrate that the proposed MOMSOA can obtain more uniform Pareto fronts (PFs) and optimal best compromise solution (BCS). Finally, two metrics that measure the performance of multi-objective algorithms, *SP* and *HV*, are employed to evaluate the results of each algorithm, and the results reveal that solutions obtained by MOMSOA are the most uniform, with the broadest diversity and the best convergence.**

Manuscript received September 29, 2022; revised January 5, 2023. This work was supported by the National Natural Science Foundation of China under Grant 51207064.

Gonggui Chen is a professor of Key Laboratory of Industrial Internet of Things and Networked Control, Ministry of Education, Chongqing University of Posts and Telecommunications, Chongqing 400065, China; (e-mail: chenggpower@ 126.com).

Tao Tan is a graduate student of Chongqing University of Posts and Telecommunications, Chongqing 400065, China (e-mail:ttcqupt@163.com).

Wei Xiang is a senior engineer of the Economic and Technology Research Institute, State Grid Chongqing Electric Power Company, Chongqing 401120, China (e-mail: weixiang_cq@163.com).

Zhenqi Guan is a senior engineer of the Economic and Technology Research Institute, State Grid Chongqing Electric Power Company, Chongqing 401120, China (e-mail: zhenqiguan_cq@163.com).

Hao Tan is a senior engineer of the Economic and Technology Research Institute, State Grid Chongqing Electric Power Company, Chongqing 401120, China (e-mail: tanhao_cq@163.com).

Jianbo Yu is a senior engineer of the Economic and Technology Research Institute, State Grid Chongqing Electric Power Company, Chongqing 401120, China (e-mail: jianboyu_cq@163.com).

Hongyu Long* is a professor level senior engineer of Chongqing Key Laboratory of Complex Systems and Bionic Control, Chongqing University of Posts and Telecommunications, Chongqing 400065, China (corresponding author to provide phone: +8613996108500; e-mail: longhongyu20@163.com).

***Index Terms*—EED, MOSOA, constraint handling approach, non-inferior sorting.**

I. Introduction

With the growth of global trade and rapid economic development, the scale of various industries has been growing, and the demand for electricity for residential and industrial use has increased dramatically. However, the main source of electric energy is thermal power generation, which will consume large amounts of non-renewable resources such as coal. Therefore, how to improve the power quality, stability and economy of the power system is receiving more and more attention [1-3].

Dealing with the problem between the input and output of power system has been a classical problem in optimization field. As the basic and core problem of optimal power system operation, economic load dispatch (ELD) technology has received continuous attention from scholars and technicians in earlier studies. The essence of ELD is to meet various load demands and optimize the economic efficiency of the system by reasonably scheduling and arranging the operation of power sources under the premise of technical and safety constraints of the power system. The optimization scheme of ELD is directly related to the balance of power supply and demand, which is of great practical importance for ensuring the safe and economic, energy-saving and efficient operation of power systems. Since 1930s, scholars from various countries have conducted in-depth research on the models and algorithms for the ELD problem of power systems, and fruitful results have been achieved in both theory and practice [4-8].

Nevertheless, the thermal power generation system supported by coal energy consumes a large amount of coal and other disposable energy while generating a great deal of polluting gases, which seriously affects the environmental quality [9]. In particular, air pollutants like CO_2 produced by fossil fuel combustion have a negative impact on climate and environment. As the problems of energy shortage and environmental pollution become increasingly serious, the traditional dispatch mode with single objective of economic efficiency fails to take into account the negative impact of pollution emission from fossil energy units on the environment. The novel environmental/economic power dispatch has turned into a hot research theme in power industry due to its ability to simultaneously consider environmental protection and economic benefits [10-14].

The EED optimization problem is a non-convex, non-linear, high-dimensional, multi-objective optimization problem with many constraints, where multiple objective functions are contradictory, and a decrease in one will inevitably cause an increase in another [15, 16]. Therefore, it has an important relevance to find a balance point to maximize the common interests. Traditional mathematical optimization algorithms, such as linear weighting method, objective weighting method, will have non-feasible solutions in the solving process as well as consume long operation time, which makes it more difficult to handle high-dimensional and non-convex optimization problems like EED [17].

In recent years, benefiting from the fast development of intelligent algorithms, heuristic algorithms have been widely used in EED with excellent performance. These representative algorithms are particle swarm optimization (PSO), differential evolution (DE), artificial bee colony (ABC), non-dominant sorting genetic algorithm (NSGA), Firefly algorithm (FA), etc [18-21]. After Gaurav Dhiman and Vijay kumar proposed the seagull optimization algorithm (SOA) in 2019, it is widely adopted for diverse optimization areas [22]. In literature [23], a modified seagull optimization technique is utilized to minimize the generation cost of grid-connected hybrid renewable energy systems. In literature [24], a multi-objective seagull algorithm incorporating non-inferior ranking was employed to simultaneously optimize economic, energy, and environmental objectives in the operation of combined cooling, heating, and power system with satisfactory performance. In literature [25], the improved TISOA in combination with the whale optimization algorithm is applied to power transformer fault diagnosis. In literature [26], the modified ISOA is used to seek the optimal coordination of Distance and Directional Over-Current Relays with great complexity and many constraints. In literature [27], the two-point heading rule is combined with the seagull optimization algorithm to obtain SEOA applied to optimize the operation of this multi-reservoir system to increase the power generation.

With the widespread application of SOA, multi-objective seagull optimization (MOSOA), which deals with multi-objective optimization, is also proposed with simple structure, easy operation and high efficiency [28]. However, the algorithm suffers from the shortcomings of easily falling into local optimum, slow convergence and inability to balance global and local search. Regarding the drawback of convergence speed, logistic map is utilized to randomize the parameter u and to increase the diversity of the spiral radius thus speeding up the convergence speed. In addition, the attack phase is improved by combining mutation operator, which enables the algorithm to search more regions and effectively avoid local optimal. Moreover, the parameter A combined cosine non-linear dynamic change strategy is adopted to balance the exploration capacity and exploitation capacity of MOSOA. The combination of proposed constraint treatment and non-inferior sorting strategy is sufficient to gain more uniformly distributed POS. In summary, the multi-objective modified seagull optimization algorithm (MOMSOA) is eventually acquired.

Applied to three test systems of different scales including IEEE30-Bus, IEEE57-Bus and IEEE118-Bus systems, MOMSOA was compared with MOPSO/MODE and MOSOA to verify its effectiveness. As a complement, two metrics used to measure multi-objective algorithms, *SP* and *HV*, are applied to evaluate the degree of uniformity, convergence and diversity of the results from algorithms [29-31].

The organization of the paper is as below: section II provides mathematical description of the EED problems, and Section III focuses on MOSOA and all measures of improvements. Section IV contains the analysis of the results from all experiments as well as the analysis of performance metrics. The conclusion is given in Section V.

II. Statement of EED Problems

The EED aims to obtain the lowest cost and the minimum pollution emission in the case of satisfying numerous equality and inequality constraints [32]. Meanwhile, the power loss on transmission lines inevitably has great impact on economical and stable operation of power systems. Therefore, the power loss of is also one of the optimization objectives of the EED. The mathematical description of the EED is as below:

$$\text{minimize } F = (f_1(\mathrm{G}_i), f_2(\mathrm{G}_i), \cdots f_M(\mathrm{G}_i)) \tag{1}$$

$$\begin{aligned} g_j(\mathrm{G}_i) \geq 0, \quad j = 1, 2, \cdots, \mathrm{m} \\ h_k(G_i) = 0, \quad k = 1, 2, \cdots, \mathrm{n} \end{aligned} \tag{2}$$

where $f_1(G_i)$, $f_2(G_i)$ and $f_M(G_i)$ are objective functions, M is the ordinal number for the objectives, G_i stands for the active output power of generator, m and n stand for total number of equality and inequality constraints.

The optimization of EED must meet equality and inequality constraints, and its mathematical description has the following two main parts: objective functions as well as many constraints. The objectives specifically refer to fuel cost, pollution emission, and system power loss.

A. Objective Functions

1) Minimize fuel cost

Fuel cost is linked to economic operation in power systems, and the fuel cost of each unit is described as a quadratic function of the unit's active power.

$$M_{Fcost} = \sum_{k=1}^{N} (a_k + b_k P_{Gk} + c_k P_{Gk}^2) \ (\$/\mathrm{hr}) \tag{3}$$

where M_{Fcost} denotes total cost, a_k, b_k and c_k are the cost coefficients.

For large thermal generating units, the plucking phenomenon caused by the sudden opening of the turbine inlet valve will superimpose a pulsation effect on the generator consumption curve, which is valve point effect. The presence of valve point effect, which makes the consumption characteristic curve uneven, leads to the increase of energy consumption and results in a certain degree of impact on the economic cost. In contrast to the case without valve point effect, a sine function is added to original mathematical model of fuel cost, which will obviously affect the accuracy of solving the cost objective function if the change of units consumption characteristics is ignored [33, 34]. The presence of the valve point effect makes the objective more complex and difficult to optimize.

$$M_{Fcost-vp} = \sum_{k=1}^{N} (a_k + b_k P_{Gk} + c_k P_{Gk}^2 + \left| d_k \times \sin(e_k \times (P_{Gk}^{\min} - P_{Gk})) \right|) (\$/\mathrm{hr}) \tag{4}$$

where d_k and e_k represent fuel cost coefficients with valve point effect, P_{Gk}^{min} is the lowest limit of active power output of the kth thermal generator.

2) Minimize pollution emission

Conventional thermal power generating units produce air pollutants such as CO_2, NO_x and SO_x during their operation. A combination of quadratic and exponential functions is generally used to represent pollutant emission, the amount of which is linked to the actual power from thermal power units.

$$M_{\text{Emission}} = \sum_{k=1}^{N} \alpha_k + \beta_k P_{Gk} + \gamma_k P_{Gk}^2 + \zeta_k \exp(\lambda_k P_{Gk}) (\text{ton/hr}) \tag{5}$$

where α_k, β_k, γ_k, ζ_k and λ_k denote the emission coefficients of the kth generator.

3) Minimize power loss

During the transmission of electricity, on the one hand, transmission losses are inevitable, on the other hand, power loss will adversely influence economy and safety in power system. Therefore, it is of great significance to optimize this objective.

$$M_{Ploss} = \sum_{j}^{NB} \sum_{k \neq j}^{NB} g_{jk} \left[V_j^2 + V_k^2 - 2V_j V_k \cos \delta_{jk} \right] (\text{MW}) \tag{6}$$

where NB refers to the total quantity of buses; j and k refer to sequence numbers of buses; g_{jk} represents the conductance between bus j and bus k; V_j and V_k indicate the voltage of buses j and k; δ_{jk} is the difference of voltage phase angle between buses j and k.

B. System Constraints

1) Equality constraints

The generator output power must satisfy both load demand and network losses, which can be expressed as:

$$\sum_{j=1}^{N} P_{Gk} = P_D + P_{loss} \tag{7}$$

The output power is further divided into two parts: active power and reactive power, which needs to meet following equality constraints:

$$\begin{aligned} P_{Gj} - P_{Dj} - V_j \sum_{k=1}^{NB} V_k (G_{jk} \cos \delta_{jk} + B_{jk} \sin \delta_{jk}) = 0 \qquad j \in N \\ Q_{Gj} - Q_{Dj} - V_j \sum_{k=1}^{NB} V_k (G_{jk} \sin \delta_{jk} - B_{jk} \cos \delta_{jk}) = 0 \qquad j \in N_{pq} \end{aligned} \tag{8}$$

where P_{Gj} and Q_{Gj} represent the active and reactive power injected at node j, respectively; N_{pq} indicates the quantity of PQ buses; P_{Dj} and Q_{Dj} correspond to actual active power as well as reactive power of bus k; G_{jk} and B_{jk} represent conductance and susceptance between two nodes j and k, respectively.

2) Inequality constraints

The second type of constraint is the inequality constraint including active power, reactive power, bus voltage and power flow, which must be satisfied to guarantee safe and economical operation. They can be mathematically described as follows:

(i) Active power constraint

$$P_j^{\min} \le P_j \le P_j^{\max} \tag{9}$$

(ii) Reactive power constraint

$$Q_{Gj}^{\min} \le Q_{Gj} \le Q_{Gj}^{\max} \tag{10}$$

(iii) Bus voltage constraint

$$V_j^{\min} \le V_j \le V_j^{\max} \tag{11}$$

As each line has its limit capacity, line flow constraint is also necessary for safe and stable operation of power systems.

$$P_{lf,j} \mid \le P_{lf,j}^{\max} \qquad j \in l \tag{12}$$

where $P_{lf,j}$ represents the actual active power transmitted by line j, $P_{lf,j}^{max}$ is the maximum active power of line j , and l denotes the total quantity of lines.

III. Proposed Modified Method

A. Introduction of MOSOA

Seagull optimization algorithm (SOA), a new population intelligence algorithm proposed by Gaurav Dhiman and Vijay kumar in 2019, mainly simulates migration of seagulls in nature and aggressive behavior (foraging behavior) during the migration. Seagulls are a worldwide flock of seabirds that migrate between different geographic regions in search of food with the seasonal changes. The feeding process of seagulls consists of migration phase and predation phase: during the migration phase, seagulls follow a certain pattern to maintain individual flight independence and to avoid collision; throughout the predation phase, seagulls attack their prey in the form of spiral flight.

1) Migration behavior (exploration Process)

Individuals explore from one location to another in the migratory behavior of seagulls. In this phase, three aspects need to be taken care of: avoiding collisions, moving closer to the optimal individual and maintaining close contact with the optimal agent. To prevent collision among seagulls, the algorithm adjusts seagulls' positions by using additional variable A.

$$C_S(t) = A_s * P_s(t) \tag{13}$$

where $P_s(t)$ refers to current position of the individual seagull, $C_s(t)$ denotes the new position without position conflict with other seagull individuals, t represents current number of iterations, A denotes the motion behavior in specified space, which is mathematically described as follows:

$$A = f_c (1 - t / t_{\max}) \tag{14}$$

where f_c is the control factor set to constant 2. t_{max} denotes the maximum number of iterations.

When guaranteeing there will be no collision, seagulls converge towards the optimal seagull. The mathematical model is as below:

$$M_s(t) = B * (g_{best}(t) - P_s(t)) \tag{15}$$

where $M_s(t)$ refers to convergence direction of the individual towards the best individual, $g_{best}(t)$ is the best current position, B serves as a crucial parameter for balancing exploration and exploitation capabilities, the variation of which adheres to:

$$B = 2 * A^2 * r \tag{16}$$

where r indicates a random number between 0 and 1.

When obtaining the orientation of convergence, each seagull starts to approach towards this position:

$$D_s(t) = \left| C_s(t) + M_s(t) \right| \tag{17}$$

where $D_s(t)$ refers to the new position of individual seagull.

2) Attack behavior (exploitation process)

Moving through the air by constantly changing their angle and radius, seagulls attack the prey by descending in a spiral. e is the base of natural logarithm. The position of seagull in the three-dimensional space is:

$$x = r * \cos(k) \tag{18}$$

$$y = r * \sin(k) \tag{19}$$

$$z = r * k \tag{20}$$

$$r = u * e^{kv} \tag{21}$$

where k is a random number from 0 to 2π, u and v are the constants associated with spiral shape.

The final position is as follows:

$$P_s(t) = (D_s(t) * x * y * z) + g_{best}(t) \tag{22}$$

B. MOMSOA

1) logistic map

According to equation (13), the current individual does not have position conflict with other individuals, which can ensure the population diversity. But in equation (18-21), since the radius of spiral flight is largely determined by u that is a deterministic value, the problem of individual collision during the spiral flight inevitably arises, which makes the algorithm fall into local optimum.

In mathematical terms, chaos is the randomness of a simple deterministic dynamical system, and chaotic systems can be considered as the source of randomness. The parameters of the metaheuristic optimization algorithm are generally initialized using random variables. It is worth noting that the use of chaotic sequences to replace random variables in the chaotic gray wolf algorithm [35] can prevent optimization algorithm from local optima, inspired by it, this paper uses logical map to randomize u in each iteration, which can increase the diversity of spiral radius and effectively avoid the individual collision problem. u is generated according to:

$$u_{n+1} = u_n + \mu * (1 - u_n) \tag{23}$$

where u_{n+1} is the final value of u, u_n is a random number from 0 to 1, and μ indicates the logistic number taken as 4.

2) Mutation operator

In initial seagull algorithm, the method, by which position updates in the attack phase, is as shown in equation (22). It can be seen from equation (22) that seagulls, after migration, search for attack position according to the given action model based on the migrated position. Due to the boundedness of the action model, the seagulls may move with a dead angle of flight, which will lead to the possibility of missing the optimal position. In other words, the optimal value cannot be found during the search process, on the contrary, local optimal value will be obtained. To solve this problem, the mutant process of differential evolution is introduced. The improved location update method allows seagulls to update their location differently according to the threshold value, enabling them to search more areas. Two different position updating methods are alternated to narrow the dead angle of seagull flight and to reduce the flight blindness. Different results will be obtained in different ways, meanwhile, the optimal position will be updated in diverse angles, which increases the diversity of MOSOA. The mutation operator is described as below:

$$P_s(t) = x_{r1}(t) + F * (x_{r2}(t) - x_{r3}(t)) \tag{24}$$

where $x_{r1}(t)$, $x_{r2}(t)$, $x_{r3}(t)$ are three mutually exclusive individuals randomly selected in the population, F is the weighting factor taken as 0.6.

The improved attack method is as follows：

$$\begin{cases} P_s(t) = x_{r1}(t) + F * (x_{r2}(t) - x_{r3}(t)) & rand > a \\ P_s(t) = (D_s(t) * x * y * z) + g_{best}(t) & rand \le a \end{cases} \tag{25}$$

After several experiments, the algorithm obtains the best search performance when a is taken as 0.8.

3) Non-linear parameter A with cosine dynamic variation strategy

In MOSOA, the migration behavior of individual gulls is a significant operation of MOSOA, and A in equation (15) is an important parameter controlling the location of seagulls, which plays a crucial character in balancing the exploration and exploitation capabilities in search process. In equation (14), A changes linearly throughout operation process. On the contrary, the search process is very complex and presents a non-linear downward trend when dealing with the EED problems, which requires a nonlinear change in the exploration and exploitation behavior in order to avoid locally optimal solutions. If the control parameter A purely simulates the migration process of the seagull population in a linearly decreasing manner, the global search ability of the algorithm will be reduced, so we propose the strategy based on cosine dynamic change, whose variation follows equation (26). With this strategy, A can keep a large value and change slowly in the early stage of iteration to expand the search range of seagulls in the population, and in the later stage, parameter A keeps a small value after a sharp decrease in the mid-term search process to strengthen the accurate exploitation of the individual region. By this way, the ability of MOSOA to seek global optimal solution is greatly improved.

$$A = A_{\min} + (A_{\max} - A_{\min}) * \cos(\frac{\pi t}{t_{\max}}) \tag{26}$$

where A_{max} is taken as 2 and A_{min} is taken as 0.

4) Constraint processing strategy

■ *Control variable and state variable*

When dealing with the EED problems, the individual may violate the control variable inequality constraint (generator output active power). The following technique is used to correct the individual：

$$G_j = \begin{cases} G_{min} & if\ \ G_j < G_{min} \\ G_{max} & if\ \ G_j > G_{max} \\ G_J & if\ \ G_{min} < G_j < G_{max} \end{cases} \tag{27}$$

When the individual violated state variable inequality constraints the total violated constraint value can be expressed as:

$$total - constrvio(P_g) = \sum_k \max(g_k(P_g, x), 0) \tag{28}$$

where *total-constrvio*(P_g) represents violation value of variable inequality. $g_k(P_g, x)$ indicates the kth constraint violation value involved in state variable inequality constraint.

By calculating the individual violation constraint values, the following strategy is used to identify the dominance among individuals.

Constraint Handling Approach:

if *total-constrvio* (p_j) < *total-constrvio* (p_k)
  p_j is superior to p_k;
if *total-constrvio* (p_j) > *total-constrvio* ((p_k)
  p_k is superior to p_j;
if *total-constrvio* (p_j) = *total-constrvio* (p_k)
if $f_m(p_j) \leq f_m(p_k)$ for every $m \in [1, M]$
and $f_n(p_j) < f_n(p_k)$ for any $n \in [1, M]$
  p_j dominates p_k;
else
  p_j is inferior to p_k.

By comparing the priority of individuals through the dominant rule described above, all individuals are finally separated into *m* levels and every level is called *rank*(*j*). A smaller rank means its higher priority. For the case that there will be several individuals with equal rank, the following method was introduced.

■ *Non-inferior sorting based on crowding distance*

In view of that the same rank will have several individuals, the non-inferior sorting proposed by Deb [36] is applied to determine the priority of individuals by calculating the crowding distance. A larger crowding distance indicates a higher priority.

Constraint Handling Approach:

if *rank*(x_j) < *rank*(x_k) *j* is superior to *k*.;
if *rank*(x_k) > *rank*(x_j) *k* is superior to *j*.;
if *rank*(x_j) == *rank*(x_k)
  if *distance*(x_j) > *distance*(x_k)
  j is superior to *k*;
  else
  k is superior to *j*.

After integrating the above methods into MOSOA, MOMSOA was obtained. MOMSOA has been enhanced with the ability to efficiently handle multi-dimensional and multi-objective problems, whose pseudo code is shown below：

Initialize MOMSOA;
Input population size *N*, weighting factor *F* and max number of interations t_{max};
Identify the global optimal individual g_{best} by constraint handling strategy and non-inferior sorting;
  while $t<t_{max}$;
    for $i = 1: N$
Calculate $C_s(t)$ $M_s(t)$, $D_s(t)$, *x*, *y* and *z* by equation (13-21);
      if *rand*>*a*
        $P_s(t) = (D_s(t) * x * y * z) + g_{best}(t)$;
      else
        $P_s(t) = x(r_1) + F * (x(r_2) - x(r_3))$;
      end if
    end for
  end while
Update g_{best} using constraint handling strategy and non-inferior sorting;
if $newg_{best}$ dominate g_{best}
  $g_{best} = newg_{best}$;
else
  g_{best} remains unchanged;
end if
Obtain the final Pareto fronts and BCS;
$t = t + 1$;
end while

In order to verify the efficiency of MONSOA, it is applied to deal with the EED problems. Combining the above constraint processing strategies, a set of mutually non-dominated Pareto solution sets can be obtained. At the end of the iteration, the optimal one in *rank* (*1*) is selected as the best compromise solution. The flow of MOMSOA for the EED problems is given in Fig. 1.

IV. Experiments And Results

Based on MATLAB 2021a and a PC with Intel(R) Core (TM) i5-7500 CPU @ 3.4GHz with 16GB RAM, three test systems consisting of IEEE30-Bus, IEEE57-Bus and IEEE118-Bus systems are employed in the experiments including eight cases to demonstrate the efficiency of the proposed algorithm in dealing with the EED problems.

A. Simulation parameters and test systems

Due to the high complexity of the EED problems, the setting of any parameter will directly affect the algorithm's ability to find the optimal solution. Therefore, the setting of each parameter is crucial. The detailed parameter settings of the three algorithms MOSOA, MOPSO and MODE that were made for comparison can be found in the literature [1, 2].

Three test systems of diverse scales are employed in the simulation experiments of each algorithm, among which the IEEE30-Bus test system is the simplest one with the structure shown in Fig. 2. IEEE30-Bus system contains six generators and a range of other supporting equipment. TABLE. I shows the specific values of each parameter used to calculate the objective functions. The various data such as node data are given in the literature [37, 38].

The components of IEEE57-Bus system are slightly more complicated, which possesses seven generator units. The cost and emission coefficients are in literature [39] and the detailed information is in literature [36]. The components of IEEE57 are showed in Fig. 3.

The IEEE118 is the largest and most complex one of the three test systems with 54 generators and a series of other devices, and its structure is presented in Fig. 4. More data about system is given in literature [40].

B. IEEE 30-Bus test system

1) Case1: Optimization trial for M_{Fcost} and $M_{Emission}$

In Case 1, emission and fuel cost are optimized simultaneously. The Pareto fronts resulting from the optimization of MOMSOA, MOSOA, and MOPSO are showed in Fig. 5. It is clear that MOMSOA gains more uniformly distributed PF. In addition, the Pareto front obtained by MOMSOA is given in Fig. 6 with indicating the BCS and the minimum value solutions of optimized objectives.

The detailed data of the BCS from several algorithms is shown in TABLE. II. Meanwhile, the results from the published literature are also provided. The BCS obtained by MOMSOA is 0.1972 (ton/hr) and 621.05 ($/hr), which is superior to all the compared algorithms. The extreme value solutions of two optimization objectives from algorithms we use are listed in TABLE. III and TABLE. IV, respectively.

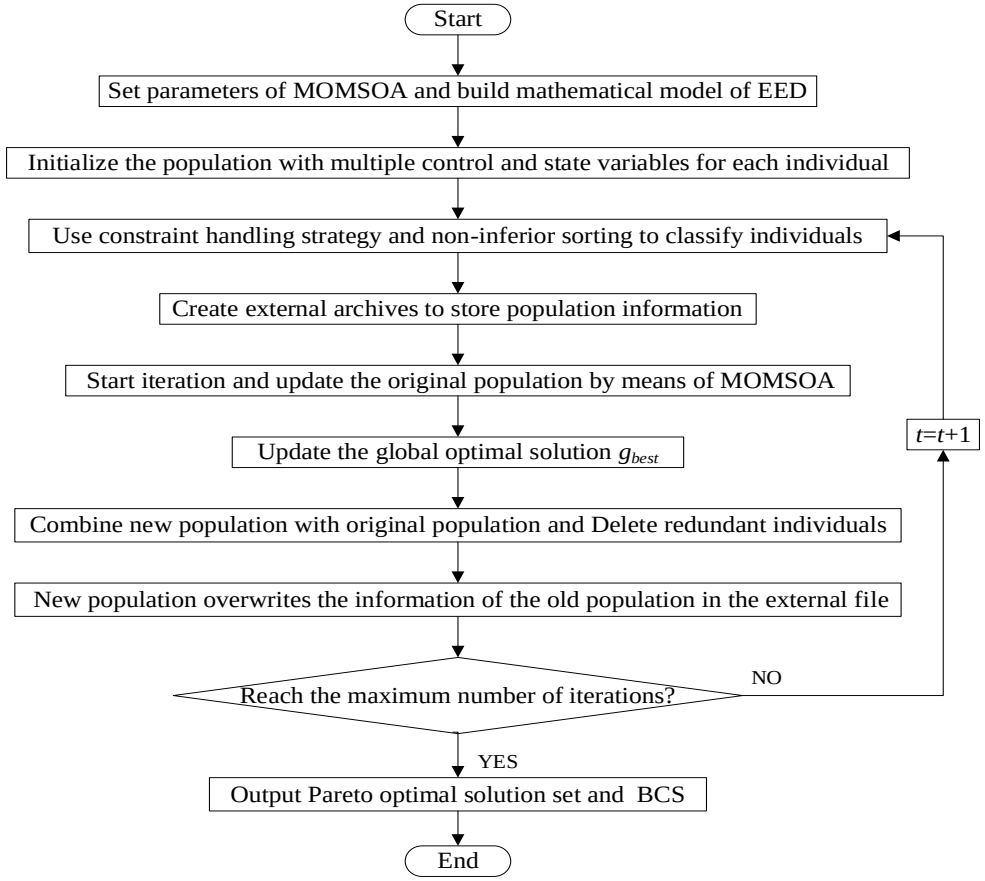

Fig. 1 Process of MOMSOA to solve EED problems

By comparing with published literature, the solutions of 610.91 ($/hr) and 0.1942 (ton/hr) obtained by MOMSOA are the lowest, which further proves its powerful optimization ability.

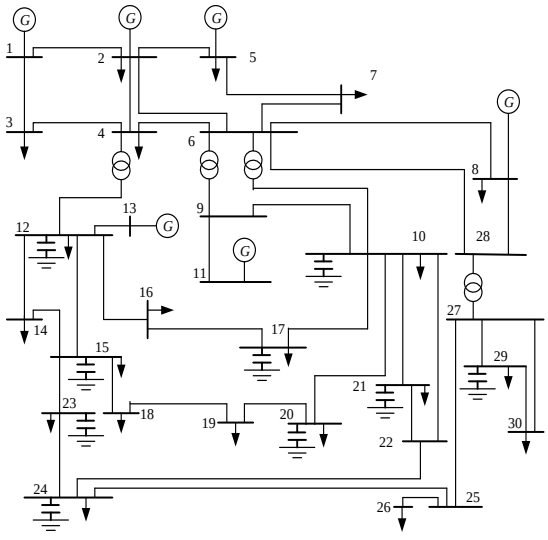

Fig. 2 Overall components for IEEE 30

2) Case2: Optimization experiment of $M_{Fcost\text{-}vp}$ and $M_{Emission}$

The existence of the valve point effect makes the objective function more complex and difficult to optimize, which further challenges the algorithm's optimization ability. Case 2 aims to optimize fuel cost with valve point effect and emission. The Pareto fronts gained by the three algorithms are provided in Fig. 7. It is obvious that MOMSOA obtains the optimal solution set. Fig. 8 shows the PF from MOMSOA and marks BCS and extreme value solutions. For comparison purposes, the BCS solutions and specific generator output data obtained by several methods including methods from published literature are listed in TABLE. VI. The BCS consisting of 637.31 ($/hr) and 0.1965 (ton/hr) from the proposed MOMSOA dominates others. As a complement, the extreme solutions obtained by the three algorithms and published literature have been listed in TABLE. V, where the lowest solutions of 624.34 ($/hr) and 0.1942 (ton/hr) are obtained by MOMSOA. The above results demonstrate that MOMSOA is capable of obtaining satisfactory solutions despite the target becomes difficult to optimize.

3) Case3: Optimization trial for $M_{Emission}$ and M_{Ploss}

The network loss is inseparable from economy and security in power system. Hence, it is essential to optimize power losses as well. In Case 3, both emission and network loss are optimized. Fig. 9 presents the Pareto fronts obtained for MONSOA, MOSOA and MOPSO. It is evident that the distribution of Pareto front obtained by MONSOA is more uniform. Fig. 10 indicates individual Pareto front of MOMSOA and marks BCS as well as extreme value solutions. For convenient comparison, TABLE. VII brings several algorithms' BCS including the BCS from the published literature. The BCS from MOMSOA is 1.3833 (MW) and 0.1998 (ton/hr), which dominates others. The extreme solutions obtained by each algorithm are similarly offered in TABLE. VIII, where the proposed MOMSOA still yields the best solutions that are 1.0830 (MW) and 0.1942 (ton/hr). All the above proves the excellent optimization capability of MOMSOA.

C. *Inspection of IEEE57-Bus system*

1) *Case4: Optimization trial for M_{Fcost} and $M_{Emission}$*

IEEE57 node system is a bit more complex than the IEEE30 node system, which leads to a greater examination of the algorithm's ability to find the optimal solution. The Pareto fronts obtained by three algorithms are illustrated in Fig. 11. The Pareto front obtained by MOMSOA is given in Fig. 12. Regretfully it is difficult for us to directly observe their dominant relationship. Therefore, local magnification is needed in this image. By this way, we can clearly notice that the Pareto front from MOMSOA is be superior to others. Furthermore, TABLE. IX shows the detailed data of the BCS from three algorithms. The BCS derived from MOMSOA is 43103.85 ($/hr) and 1.2607 (ton/hr), which dominates the other two algorithms. The boundary solutions gained by algorithms are summarized in TABLE. X, where the boundary solutions from MOMSOA are 41634.04 ($/hr) and 1.0324 (ton/hr). The results demonstrate the obvious advantages of MOMSOA to deal with EED problems.

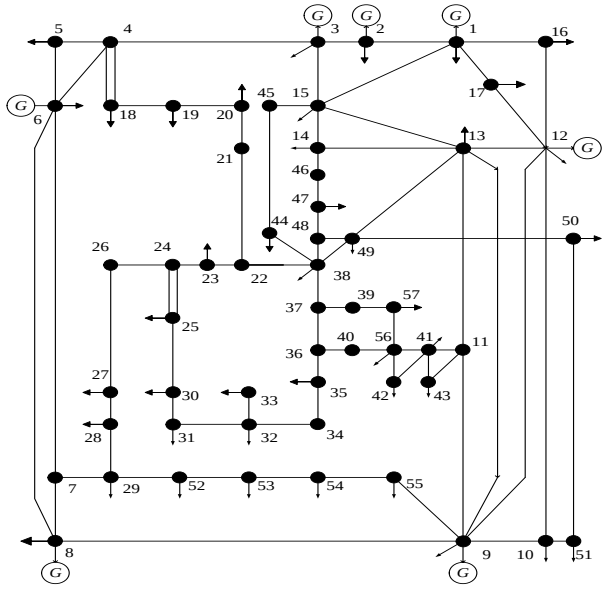

Fig. 3 Overall components for IEEE 57

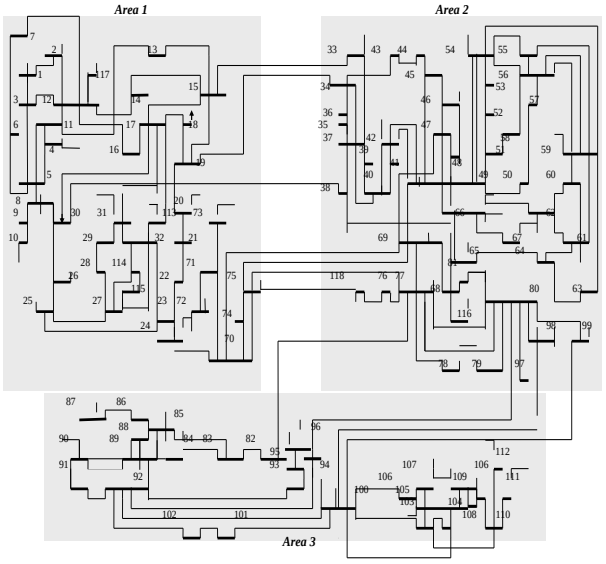

Fig. 4 Overall components for IEEE 118

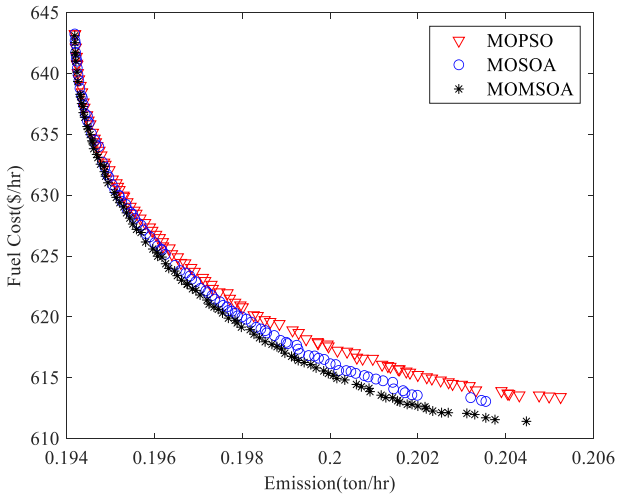

Fig. 5. Pareto fronts for Case 1

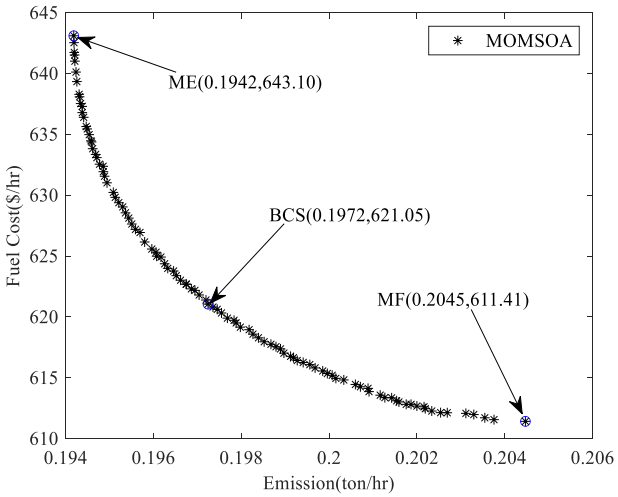

Fig. 6. Individual Pareto front of MOMSOA for Case 1

TABLE. I
GENERATOR AND EMISSION COEFFICIENTS

NO.	α	β	γ	ζ	λ	P_{min}	P_{max}	a	b	c
$Gen_{\_1}$	0.04091	-0.05554	0.06490	0.0002	2.857	5	150	10	200	100
$Gen_{\_2}$	0.02543	-0.06047	0.05638	0.0005	3.333	5	150	10	150	120
$Gen_{\_5}$	0.04258	-0.05094	0.04586	0.000001	8.000	5	150	20	180	40
$Gen_{\_8}$	0.05326	-0.03550	0.03380	0.002	2.000	5	150	10	100	60
$Gen_{\_11}$	0.04258	-0.05094	0.04586	0.000001	8.000	5	150	20	180	40
$Gen_{\_13}$	0.06131	-0.05555	0.05151	0.00001	6.667	5	150	10	150	100

TABLE. II
OBTAINED BCS RESULTS OF CASE 1

Output	MOMSOA	MOSOA	MOPSO	MONTSA[1]	MONWOA[2]	SPEA[41]	MBFA[42]	MOPSO[43]	DE[44]	NSGA-II[45]
Gen_1(MW)	0.3070	0.2917	0.2713	0.3085	0.3064	0.3052	0.2983	0.2882	0.3877	-
Gen_2(MW)	0.4097	0.4142	0.4052	0.4011	0.4019	0.4389	0.4332	0.3965	0.5201	-
Gen_5(MW)	0.5512	0.5741	0.6210	0.5546	0.5699	0.7163	0.7350	0.7320	0.2538	-
Gen_8(MW)	0.5976	0.5890	0.5454	0.5935	0.5890	0.6978	0.6899	0.7520	0.7281	-
Gen_{11}(MW)	0.5372	0.5400	0.5773	0.5472	0.5419	0.1552	0.1569	0.1489	0.4655	-
Gen_{13}(MW)	0.4503	0.4495	0.4321	0.4482	0.4436	0.5507	0.5503	0.5463	0.5101	-
$\boldsymbol{M_{Fcost}}$**($/hr)**	**621.05**	622.31	622.44	621.09	621.12	629.59	629.56	626.10	626.03	625.36
$\boldsymbol{M_{Emission}}$**(ton/hr)**	**0.1972**	0.1973	0.1975	0.1972	0.1972	0.2079	0.2080	0.2106	0.1979	0.1984

TABLE. III
SPECIFIC DATA OF *ME* IN CASE 1

Output	MOMSOA	MOSOA	MOPSO	MONTSA[1]	MONWOA[2]	SPEA[41]	MBFA[42]	MOPSO[43]	NSGA[46]	NSBF[47]
Gen_1(MW)	0.4094	0.4081	0.4142	0.4118	0.4113	0.3052	0.4716	0.4589	0.4403	0.4047
Gen_2(MW)	0.4604	0.4630	0.4614	0.4673	0.4574	0.4389	0.5127	0.5121	0.4940	0.4533
Gen_5(MW)	0.5383	0.5420	0.5374	0.5413	0.5398	0.7163	0.6189	0.6524	0.7509	0.5439
Gen_8(MW)	0.3908	0.3837	0.3905	0.3857	0.3934	0.6978	0.5032	0.4331	0.5060	0.3921
Gen_{11}(MW)	0.5425	0.5426	0.5437	0.5403	0.5411	0.1552	0.1788	0.1981	0.1375	0.5454
Gen_{13}(MW)	0.5145	0.5181	0.5141	0.5130	0.5143	0.5507	0.5822	0.6129	0.5364	0.5246
$\boldsymbol{M_{Fcost}}$**($/hr)**	642.94	643.93	644.46	644.48	643.0	629.59	651.93	656.87	649.24	644.41
$\boldsymbol{M_{Emission}}$**(ton/hr)**	**0.1942**	0.1942	0.1942	0.1942	0.1942	0.2079	0.2019	0.2014	0.2048	0.1942

TABLE. IV
SPECIFIC DATA OF *ME* IN CASE 1

Output	MOMSOA	MOSOA	MOPSO	MOTSA[1]	MONWOA[2]	SPEA[41]	MBFA[42]	MOPSO[43]	NSGA[46]	NSBF[47]
Gen_1(MW)	0.1690	0.1364	0.1468	0.1561	0.1569	0.1319	0.1175	0.1524	0.1358	0.1780
Gen_2(MW)	0.3352	0.3366	0.4122	0.3602	0.3625	0.3654	0.3617	0.3427	0.3151	0.3366
Gen_5(MW)	0.6578	0.6837	0.7569	0.6475	0.6220	0.7791	0.7899	0.7857	0.8418	0.7292
Gen_8(MW)	0.7070	0.6893	0.6983	0.7059	0.7089	0.9282	0.9591	1.0180	1.0431	0.5908
Gen_{11}(MW)	0.5874	0.6079	0.5297	0.5821	0.590	0.1308	0.1457	0.0995	0.0631	0.5766
Gen_{13}(MW)	0.3956	0.3992	0.3063	0.3987	0.4114	0.5292	0.4916	0.4669	0.4664	0.4474
$\boldsymbol{M_{Fcost}}$**($/hr)**	**610.91**	612.43	613.86	611.10	611.23	619.60	618.06	618.54	620.87	619.61
$\boldsymbol{M_{Emission}}$**(ton/hr)**	0.2052	0.2062	0.2080	0.2051	0.2048	0.2244	0.2264	0.2308	0.2368	0.2027

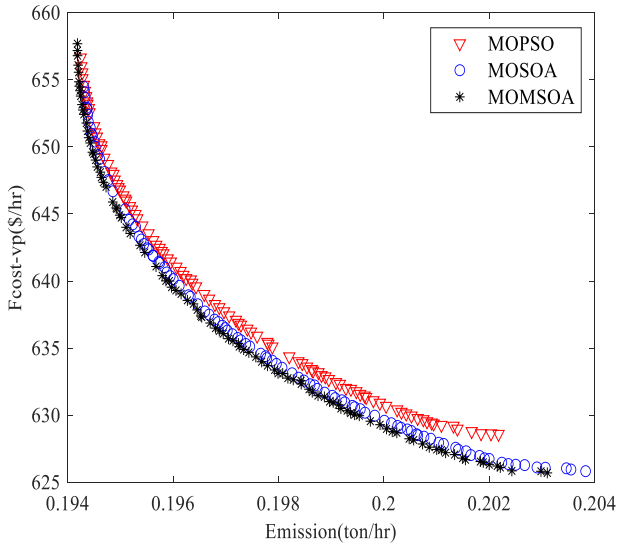

Fig. 7. Pareto fronts for Case 2

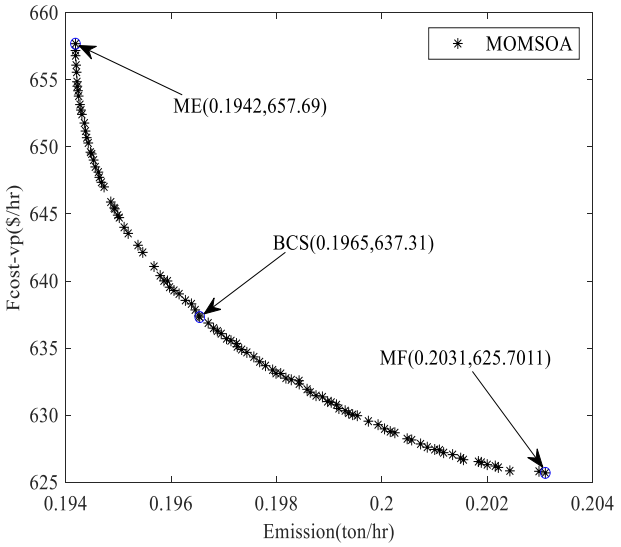

Fig. 8. Individual Pareto front of MOMSOA for Case 2

TABLE. V
SPECIFIC RESULTS ABOUT MF_{vp} AND *ME* IN CASE 2

Algorithms	Objects	Output						$\boldsymbol{M_{Fcost\text{-}vp}}$	$\boldsymbol{M_{Emission}}$
		Gen_1	Gen_2	Gen_5	Gen_8	Gen_{11}	Gen_{13}		
MOMSOA	MF_{vp}	0.1473	0.3432	0.6788	0.7079	0.5796	0.3939	**624.34**	0.2061
	ME	0.4071	0.4612	0.5447	0.3902	0.5418	0.5139	657.63	**0.1942**
MOSOA	MF_{vp}	0.1991	0.3450	0.6228	0.7042	0.5681	0.4128	625.24	0.2034
	ME	0.4122	0.4621	0.5428	0.3841	0.5413	0.5147	658.05	0.1942
MOPSO	MF_{vp}	0.2594	0.3726	0.5754	0.6840	0.5428	0.4181	627.82	0.2007
	ME	0.4093	0.4617	0.5442	0.3852	0.5395	0.5171	657.82	0.1942
MONTSA[1]	MF_{vp}	0.1805	0.3550	0.6508	0.7020	0.5396	0.4226	625.07	0.2039
	ME	0.4116	0.4631	0.5374	0.3948	0.5413	0.5173	659.21	0.1942
MONWOA[2]	MF_{vp}	0.1793	0.3643	0.5970	0.7067	0.5920	0.4136	627.12	0.2038
	ME	0.4108	0.4625	0.5438	0.3903	0.5414	0.5109	659.35	0.1942

TABLE. VI
THE BCS AND RELATED POWER OUTPUT OF CASE 2

Output	MOMSOA	MOSOA	MOPSO	MONTSA[1]	MONWOA[2]	PSO[48]
Gen_1(MW)	0.3188	0.3110	0.3585	0.3232	0.3111	0.1409
Gen_2(MW)	0.4058	0.4112	0.4288	0.4065	0.4174	0.3442
Gen_5(MW)	0.5604	0.5689	0.6048	0.5568	0.550	0.6756
Gen_8(MW)	0.5672	0.5799	0.5852	0.5700	0.5718	0.8397
Gen_{11}(MW)	0.5422	0.5213	0.5462	0.5400	0.5371	0.4904
Gen_{13}(MW)	0.4589	0.4682	0.3317	0.4568	0.4663	0.3980
$\boldsymbol{M_{Fcost\text{-}vp}}$**($/hr)**	**637.31**	638.28	638.35	637.32	638.68	639.65
$\boldsymbol{M_{Emission}}$**(ton/hr)**	**0.1965**	0.1968	0.1982	0.1965	0.1966	0.2111

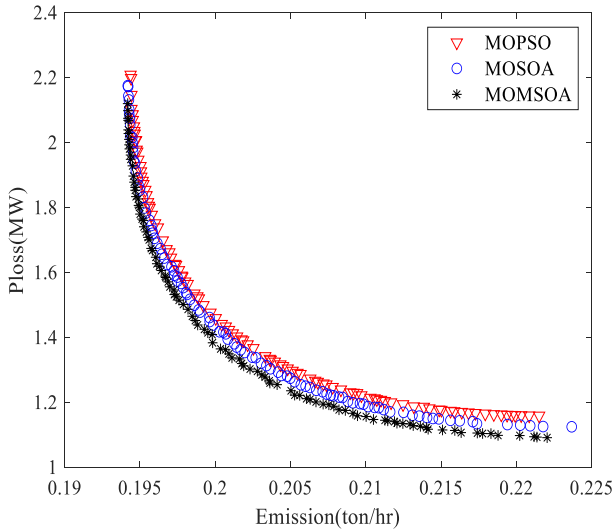

Fig. 9. Pareto fronts for Case 3

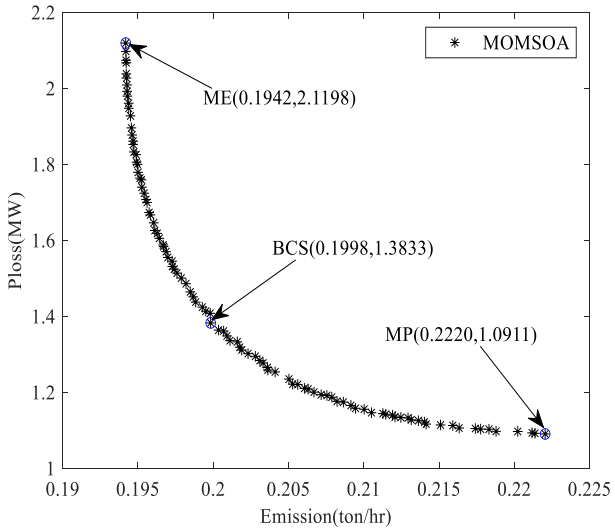

Fig. 10. Individual Pareto front of MOMSOA for Case 3

TABLE. VII
OBTAINED BCS RESULTS OF CASE 3

Output	MOMSOA	MOSOA	MOPSO	MONTSA[1]	MONWOA[2]
Gen_1(MW)	0.2553	0.2397	0.2514	0.2508	0.2202
Gen_2(MW)	0.3811	0.3642	0.3672	0.4060	0.3821
Gen_5(MW)	0.7804	0.7976	0.8074	0.7865	0.8077
Gen_8(MW)	0.4291	0.4248	0.4357	0.4050	0.4311
Gen_{11}(MW)	0.5859	0.6006	0.5945	0.5838	0.6038
Gen_{13}(MW)	0.4160	0.4210	0.3920	0.4158	0.4046
$\boldsymbol{M_{Ploss}}$**(MW)**	**1.3833**	1.3948	1.4122	1.3872	1.5496
$\boldsymbol{M_{Emission}}$**(ton/hr)**	**0.1998**	0.2008	0.2012	0.1998	0.2016

TABLE. VIII
SPECIFIC DATA OF *MP* AND *ME* IN CASE 3

Algorithms	Objects	Output						$\boldsymbol{M_{Ploss}}$	$\boldsymbol{M_{Emission}}$
		Gen_1	Gen_2	Gen_5	Gen_8	Gen_{11}	Gen_{13}		
MOMSOA	*MP*	0.3019	0.2910	1.0590	0.5019	0.6467	0.3161	**1.0830**	0.2257
	ME	0.4087	0.4668	0.5388	0.3863	0.5424	0.5125	2.1600	**0.1942**
MOSOA	*MP*	0.0804	0.3034	0.9943	0.4772	0.6354	0.3544	1.1112	0.2172
	ME	0.4106	0.4622	0.5357	0.3921	0.5369	0.5188	2.2385	0.1942
MOPSO	*MP*	0.1684	0.3583	0.8882	0.4597	0.5980	0.3734	1.2076	0.2067
	ME	0.4081	0.4587	0.5410	0.3947	0.5421	0.5128	2.3391	0.1942
MONTSA[1]	*MP*	0.0697	0.2767	1.0203	0.4946	0.6486	0.3349	1.0875	0.2207
	ME	0.4135	0.4626	0.5427	0.3868	0.5352	0.5150	2.1911	0.1942
MONWOA[2]	*MP*	0.2200	0.2964	0.8408	0.4853	0.6402	0.3636	1.2423	0.2235
	ME	0.4112	0.4623	0.5452	0.3884	0.5452	0.5079	2.6211	0.1942

TABLE. IX
OBTAINED BCS RESULTS OF CASE 4

Output	MOMSOA	MOSOA	MOPSO
Gen_1(MW)	221.82	221.21	215.29
Gen_2(MW)	99.95	100	100
Gen_3(MW)	88.52	87.72	92.04
Gen_6(MW)	100	100	99.87
Gen_8(MW)	337.50	336.18	333.98
Gen_9(MW)	100	100	100
Gen_{12}(MW)	316.01	319.70	324.76
$\boldsymbol{M_{Fcost}}$**($/hr)**	**43103.85**	43124.77	43210.80
$\boldsymbol{M_{Emission}}$**(ton/hr)**	**1.2607**	1.2674	1.2703

TABLE. X
SPECIFIC DATA OF *MF* AND *ME* IN CASE 4

Algorithms	Objects	Output							M_{Fcost}	$M_{Emission}$
		Gen_1	Gen_2	Gen_3	Gen_6	Gen_8	Gen_9	Gen_{12}		
MOMSOA	*MF*	145.95	90.26	44.58	91.08	448.10	91.82	352.89	**41634.04**	1.9661
	ME	330.53	100	140	99.97	260.03	100	240.21	48453.93	**1.0324**
MOSOA	*MF*	149.03	99.84	47.90	100	408.31	100	358.52	41716.85	1.6743
	ME	307.40	100	140	100	270.70	99.88	251.72	47594.57	1.0379
MOPSO	*MF*	159.20	100	49.45	100	394.66	100	359.98	41784.63	1.6056
	ME	307.33	100	140	100	270.70	100	252.13	47609.61	1.0388

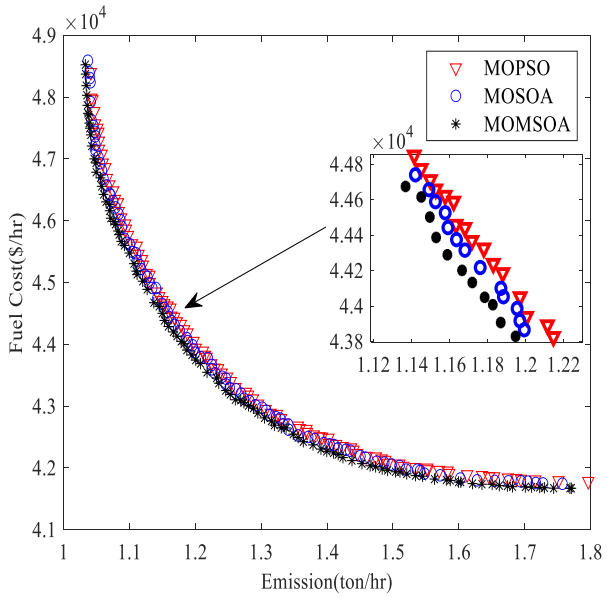

Fig. 11. Pareto fronts for Case 4

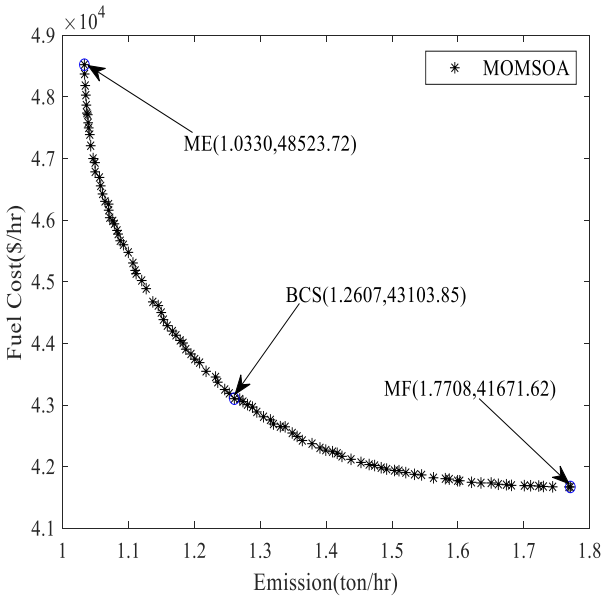

Fig. 12. Individual Pareto front of MOMSOA for Case 4

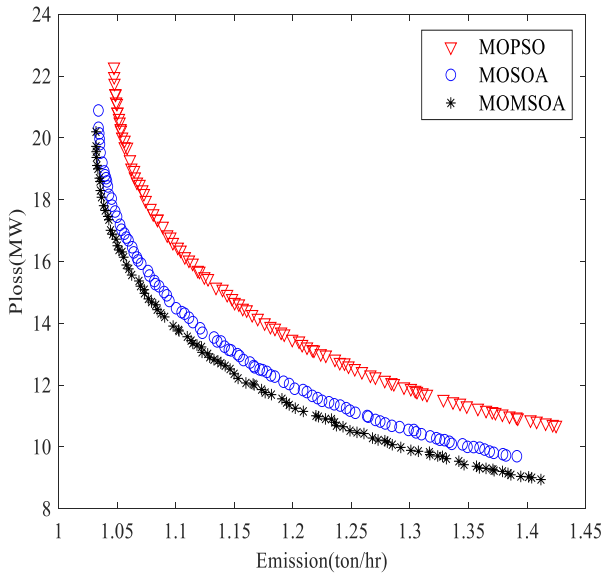

Fig. 13. Pareto fronts for Case 5

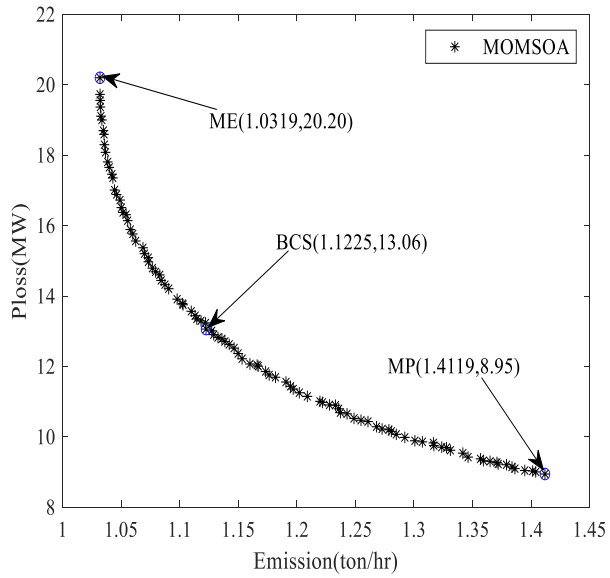

Fig. 14. Individual Pareto front of MOMSOA for Case 5

TABLE. XI
OBTAINED BCS RESULTS OF CASE 5

Output	MOMSOA	MOSOA	MOPSO
Gen_1(MW)	226.95	216.90	228.60
Gen_2(MW)	100	99.99	91.23
Gen_3(MW)	139.88	140	140
Gen_6(MW)	99.90	99.95	100
Gen_8(MW)	277.55	273.96	283.63
Gen_9(MW)	99.90	100	97.21
Gen_{12}(MW)	319.68	333.65	324.9
M_{Ploss}(MW)	**13.06**	13.65	14.78
$M_{Emission}$ (ton/hr)	**1.1224**	1.1490	1.1567

TABLE. XII
SPECIFIC DATA ABOUT *MP* AND *ME* IN CASE 5

Algorithms	Objects	Output							M_{Ploss}	$M_{Emission}$
		Gen_1	Gen_2	Gen_3	Gen_6	Gen_8	Gen_9	Gen_{12}		
MOMSOA	*MP*	187.78	18.40	139.75	99.84	304.15	99.31	410	**8.42**	1.5215
	ME	330.99	100	140	100	265.39	100	234.32	19.90	**1.0317**
MOSOA	*MP*	162.05	99.98	139.79	99.85	273.68	99.95	385.61	10.11	1.2924
	ME	317.65	100	140	99.96	261.11	99.98	250.91	18.80	1.0341
MOPSO	*MP*	181.77	100	139.87	99.98	275.06	100	364.96	10.82	1.2296
	ME	310.45	100	140	100	261.46	99.77	257.34	18.23	1.0367

2) Case5: Optimization trial for M_{Ploss} and $M_{Emission}$

After optimizing both network loss and pollution emission on the IEEE57 node system simultaneously, the Pareto fronts received from MOMSOA, MOSOA and MOPSO are presented in Fig. 13, where their differences are quite obvious. The Pareto front obtained by MOMSOA is provided in Fig. 14. It turns out that MOMSOA generates superior Pareto front. TABLE. XI shows the detailed data of the BCS obtained by every algorithm, and the BCS gained by MOMSOA is 13.06 (MW) and 1.1224 (ton/hr), which still outperforms the compared algorithms. In addition, the minimum boundary solutions from several algorithms are listed in the TABLE. XII. The boundary value solutions obtained by MOMSOA are 8.42 (MW) and 1.0317 (ton/hr), which are also the optimal. Even in the face of more complex system, MOMSOA still has certain advantages to deal with EED problems.

3) Case6: Optimization trial for $M_{Fcost\text{-}vp}$ and $M_{Emission}$

For the IEEE57 node system which is more complex than the IEEE30 node system, the optimization process will become extremely challenging when combining with the nonlinearity and discontinuity of the valve point effect. Thus Case 6 aims to simultaneously optimize $M_{Fcost\text{-}vp}$ and $M_{Emission}$. The Pareto fronts of three algorithms are represented in Fig. 15. Furthermore, the Pareto front from MOMSOA is available in Fig. 16. It is highly noteworthy that the PF from MOMSOA is pretty continuous, which is a superior performance.

The BCS of three algorithms as practical solutions are displayed in TABLE. XIII with their respective generator active outputs, and it is apparent that MOMSOA obtains the optimal BCS of 44957.14 ($/hr) and 1.1912 (ton/hr). As a supplement, the boundary solutions obtained by several algorithms are presented in TABLE. XIV, and the lowest boundary solutions, 42532.82 ($/hr) and 1.0360 (ton/hr), is still from the proposed MOMSOA. After the test of Case 6, the strong competitiveness of MOMSOA in dealing with the EED problems is once again demonstrated.

D. Inspection of IEEE118-Bus system

1) Case7: Optimization trial for M_{Fcost} and $M_{Emission}$

The IEEE118 node system is a huge and complex system containing 65 generator units. To examine the efficiency of MOMSOA in handling EED problems of large system, both fuel cost and pollution emission are optimized in Case 7. Due to the insufficient performance of MOPSO, the results do not converge even after the completion of the iterations. Therefore, the comparison algorithm is replaced with multi-objective differential evolutionary (MODE) algorithm in Case 7.

The Pareto fronts resulting from the three algorithms are presented in Fig. 17. Apparently, MOMSOA obtains a Pareto front with a wide and uniform distribution. Fig. 18 illustrates the Pareto front for MOMSOA alone as well as labels the BCS and extreme value solutions.

TABLE. XV demonstrates the BCS solutions from several algorithms and the specific values of output active power. It is undeniable that the BCS of 62880.30 ($/hr) and 1.2251 (ton/hr) obtained by MOMSOA is the optimal one. Moreover, the boundary solutions they obtained are listed in TABLE. XVI. It is the extreme value solutions of 57115.27 ($/hr) and 0.3544(ton/hr) derived from MOMSOA that are still the smallest. The excellent ability of MOMSOA to deal with the EED problems is once again demonstrated despite in the face of large and complex system.

2) Case8: Optimization trial for M_{Ploss} and $M_{Emission}$

In large systems such as IEEE118 node system, the algorithm faces a greater challenge in its ability to solve complex EED problems. To further examine the performance of MOMSOA, Case8 optimizes both emission and network loss for IEEE118 node system. The Pareto fronts from three algorithms are provided in Fig. 19, and the Pareto front obtained by MOMSOA is alone presented in Fig. 20. The difference is obvious, which proves that the proposed MOMSOA obtains the most uniform Pareto front and outperforms the other two algorithms. The BCS obtained by three algorithms are shown TABLE. XVII with detailed generator output data, and the BCS from MOMSOA, 97.15 (MW) and 0.8177 (ton/hr), is clearly the optimal solution. The boundary solutions of the two objective functions obtained by the three algorithms are also listed in TABLE. XVIII. The difference with the other cases is that MOMSOA obtained the lowest network loss of 55.06 (MW), but MODE obtained the lowest pollution emission boundary value of 0.4167 (ton/hr). The reason for this result is that the classical DE algorithm has excellent robustness. However, the remaining results still provide strong evidence of the superior ability of the proposed MOMSOA to handle EED problems in complex system.

E. Performance Indicators

As the obtained BCS and PFs are selected from the best one among 30 experiments of each algorithm. The remaining part of the results has not been utilized, consequently this section aims to quantitatively analyze each algorithm with all the experimental results. In this section, two metrics, *SP* and *HV*, are chosen to evaluate the results of the algorithm, where *SP* is applied to evaluate the uniformity of solution sets and *HV* is used to evaluate the convergence and diversity.

1) SP

The *SP* index is used to measure the standard deviation of the minimum distance from each solution to the other

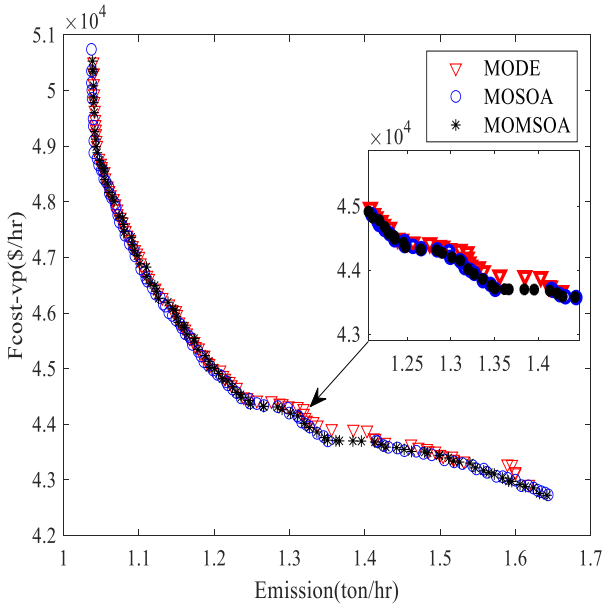

Fig. 15 Pareto fronts for Case 6

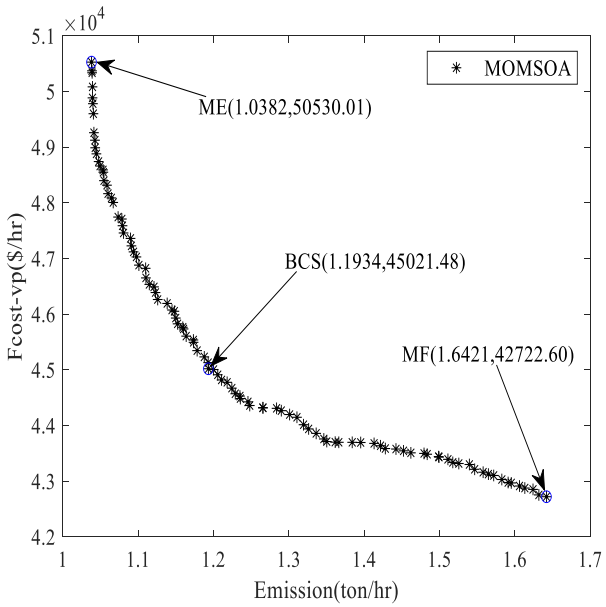

Fig. 16 Individual Pareto front of MOMSOA for Case 6

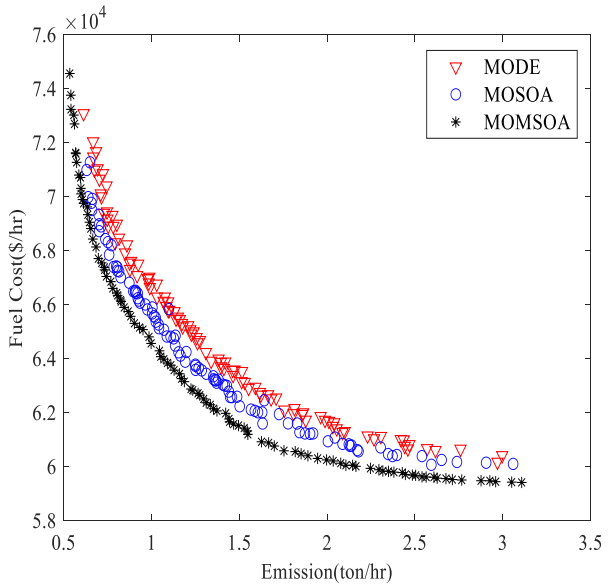

Fig. 17 Pareto fronts for Case 7

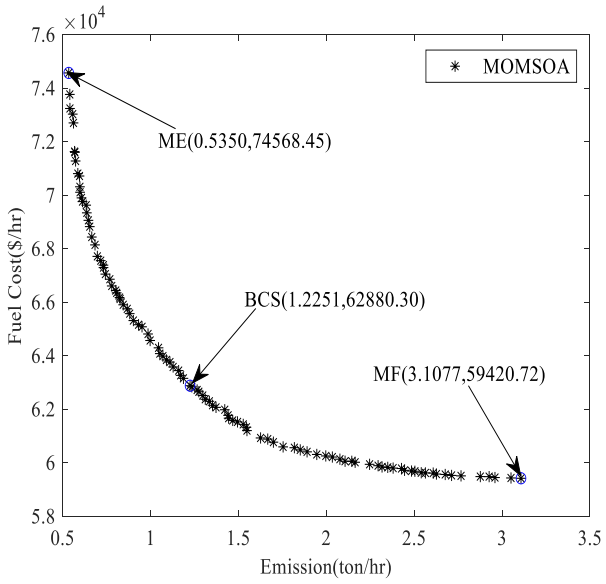

Fig. 18 Individual Pareto front of MOMSOA for Case 7

TABLE. XIII
OBTAINED BCS AND RELATED POWER OUTPUT OF CASE6

Output	MOMSOA	MOSOA	MOPSO
Gen_1(MW)	229.82	229.72	227.93
Gen_2(MW)	100	100	100
Gen_3(MW)	110.08	111.06	110.21
Gen_6(MW)	99.65	100	100
Gen_8(MW)	298.29	298.42	300.46
Gen_9(MW)	99.97	100	100
Gen_{12}(MW)	327.13	327.24	328
$M_{Fcost\text{-}vp}$($/hr)	**44957.14**	45035.81	45000.97
$M_{Emission}$(ton/hr)	**1.1912**	1.1924	1.1980

TABLE. XIV
SPECIFIC RESULTS ABOUT *MF* AND *ME* IN CASE6

Algorithms	Objects	Output							$M_{Fcost\text{-}vp}$	$M_{Emission}$
		Gen_1	Gen_2	Gen_3	Gen_6	Gen_8	Gen_9	Gen_{12}		
MOMSOA	MF_{vp}	153.36	87.11	56.17	95.71	399.82	69.90	402.20	**42532.82**	1.7919
	ME	326.71	100	140	100	266.05	99.72	239.42	50160.62	**1.0360**
MOSOA	MF_{vp}	152.93	94.68	67.19	83.95	398.94	65.03	401.78	42754.24	1.7793
	ME	228.82	96.58	100.57	99.86	350.06	100	292.33	44460.26	1.2445
MOPSO	MF_{vp}	153.15	94.50	54.00	98.24	399.08	99.86	365.90	42805.59	1.6482
	ME	328.51	100	140	99.94	262.44	100	242.4412	50255.51	1.0393

TABLE. XV
THE BCS AND RELATED POWER OUTPUT OF CASE7

Output	MOMSOA	MOSOA	MODE	Output	MOMSOA	MOSOA	MODE
Gen_4(MW)	5.11	5	6.68	Gen_{66}(MW)	100	100	100
Gen_6(MW)	5.11	5.05	8.87	Gen_{69}(MW)	-211.71	-140.82	-136.03
Gen_8(MW)	5.17	5	5	Gen_{70}(MW)	30.30	32.31	30
Gen_{10}(MW)	300	292.60	300	Gen_{72}(MW)	10.45	10	11.88
Gen_{12}(MW)	300	300	282.88	Gen_{73}(MW)	5.12	5.34	6.72
Gen_{15}(MW)	10	30	12.50	Gen_{74}(MW)	6.59	5	5
Gen_{18}(MW)	25	71.90	100	Gen_{76}(MW)	32.92	25	25.02
Gen_{19}(MW)	5	5	5	Gen_{77}(MW)	27.51	25	25
Gen_{24}(MW)	5	5	5	Gen_{80}(MW)	286.54	271.32	228.89
Gen_{25}(MW)	100.02	100	100.80	Gen_{82}(MW)	43.34	100	25
Gen_{26}(MW)	100.04	100	100	Gen_{85}(MW)	11.97	10.26	10
Gen_{27}(MW)	12.17	30	18.01	Gen_{87}(MW)	242.94	187.92	213.74
Gen_{31}(MW)	9.59	30	23.94	Gen_{89}(MW)	197.79	158.70	200
Gen_{32}(MW)	38.24	25.26	100	Gen_{90}(MW)	8.51	20	8
Gen_{34}(MW)	8	8.10	8	Gen_{91}(MW)	20.03	20	20
Gen_{36}(MW)	25	25	25.27	Gen_{92}(MW)	179.52	127.03	100
Gen_{40}(MW)	8	8	8.28	Gen_{99}(MW)	143.30	118.67	233.47
Gen_{42}(MW)	8.04	8	8	Gen_{100}(MW)	161.10	237.84	200.38
Gen_{46}(MW)	100	100	55	Gen_{103}(MW)	8.09	8.14	9.29
Gen_{49}(MW)	250	250	244.29	Gen_{104}(MW)	53.81	25	42.92
Gen_{54}(MW)	50	50	57.44	Gen_{105}(MW)	62.73	25	48.80
Gen_{55}(MW)	25	25	28.25	Gen_{107}(MW)	8.61	8.10	8.35
Gen_{56}(MW)	25.59	25	25	Gen_{110}(MW)	29.89	25	25
Gen_{59}(MW)	50.01	50	53.31	Gen_{111}(MW)	25	27.31	26.33
Gen_{61}(MW)	200	198.82	176.42	Gen_{112}(MW)	100	25.07	25
Gen_{62}(MW)	41.72	97.72	87.13	Gen_{113}(MW)	100	100	100
Gen_{65}(MW)	420	420	420	Gen_{116}(MW)	50	25	40
M_{Fcost} **($/hr)**	**62880.30**	63150.91	63191.04	$M_{Emission}$**(ton/hr)**	**1.2251**	1.3508	1.4008

TABLE. XVI
SPECIFIC RESULTS ABOUT *MF* AND *ME* IN CASE7

Algorithms	Objects	M_{Fcost}	$M_{Emission}$
MOMSOA	*MF*	**57115.27**	3.8206
	ME	77348.84	**0.3544**
MOSOA	*MF*	58532.17	3.6984
	ME	68898.35	0.7135
MODE	*MF*	60022.20	2.1428
	ME	68964.04	0.6859

TABLE. XVII
THE BCS AND RELATED POWER OUTPUT OF CASE8

Generators	MOMSOA	MOSOA	MODE	Generators	MOMSOA	MOSOA	MODE
Gen_4(MW)	29.98	24.70	30	Gen_{66}(MW)	101.41	108.84	121.97
Gen_6(MW)	29.97	30	27.25	Gen_{69}(MW)	-591.21	-563.05	30
Gen_8(MW)	30	23.92	30	Gen_{70}(MW)	38.23	62.63	12.99
Gen_{10}(MW)	299.89	299.62	277.54	Gen_{72}(MW)	10	10	12.04
Gen_{12}(MW)	299.97	299.04	300	Gen_{73}(MW)	29.56	25.15	10.01
Gen_{15}(MW)	25.26	30	26.93	Gen_{74}(MW)	20	5	25
Gen_{18}(MW)	99.54	92.26	93.81	Gen_{76}(MW)	76.81	74.79	62.02
Gen_{19}(MW)	30	5	11.83	Gen_{77}(MW)	25	25	300
Gen_{24}(MW)	5.10	7.54	7.00	Gen_{80}(MW)	300	299.01	100
Gen_{25}(MW)	101.48	100	107.80	Gen_{82}(MW)	99.61	91.18	10
Gen_{26}(MW)	100	103.02	100	Gen_{85}(MW)	18.59	19.83	100.48
Gen_{27}(MW)	8	24.39	18.17	Gen_{87}(MW)	100	107.27	200
Gen_{31}(MW)	30	26.16	30	Gen_{89}(MW)	50	50.39	9.93
Gen_{32}(MW)	99.98	98.39	100	Gen_{90}(MW)	14.26	11.06	50
Gen_{34}(MW)	8	13.91	8	Gen_{91}(MW)	38.41	20	117.27
Gen_{36}(MW)	40.37	33.50	58.40	Gen_{92}(MW)	205.95	145.69	186.57
Gen_{40}(MW)	8.72	14.55	8	Gen_{99}(MW)	168.98	251.57	141.65
Gen_{42}(MW)	12.45	24.01	13.19	Gen_{100}(MW)	201.55	248.31	8
Gen_{46}(MW)	99.27	96.94	99.58	Gen_{103}(MW)	15.77	15.74	81.22
Gen_{49}(MW)	249.79	247.21	250	Gen_{104}(MW)	100	33.91	100
Gen_{54}(MW)	50	50	51.42	Gen_{105}(MW)	25.00	67.57	8.12
Gen_{55}(MW)	25.02	25	32.73	Gen_{107}(MW)	18.76	8	50
Gen_{56}(MW)	48.86	34.65	85.86	Gen_{110}(MW)	29.63	29.22	34.88
Gen_{59}(MW)	50.98	50	50	Gen_{111}(MW)	61.78	29.21	25
Gen_{61}(MW)	194.87	199.61	200	Gen_{112}(MW)	100.00	71.08	100
Gen_{62}(MW)	99.98	98.70	100	Gen_{113}(MW)	25	96.63	44.25
Gen_{65}(MW)	419.69	415.83	415.77	Gen_{116}(MW)	49.95	46.24	30
M_{Ploss} **(MW)**	**97.15**	125.16	128.93	$M_{Emission}$**(ton/hr)**	**0.8177**	0.8432	0.8741

TABLE. XVIII
SPECIFIC RESULTS ABOUT *MF* AND *ME* IN CASE8

Algorithms	Objects	M_{Ploss}	$M_{Emission}$
MOMSOA	*MP*	**55.06**	1.7554
	ME	120.87	**0.4513**
MOSOA	*MP*	66.52	1.8861
	ME	220.32	0.5186
MODE	*MP*	73.55	2.1507
	ME	195.44	**0.4167**

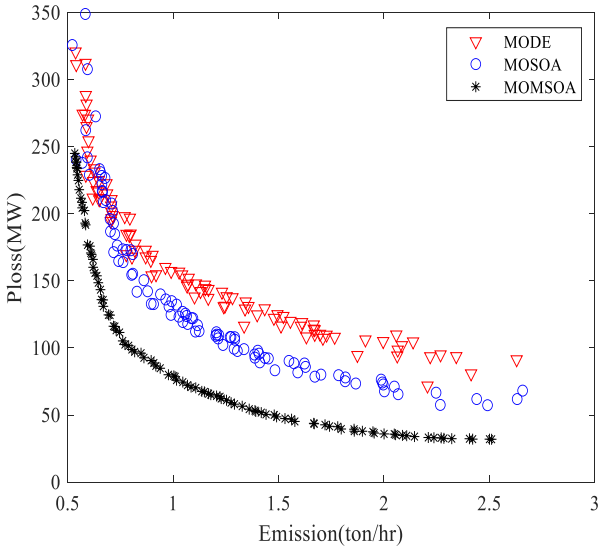

Fig. 19 Pareto fronts for Case 8

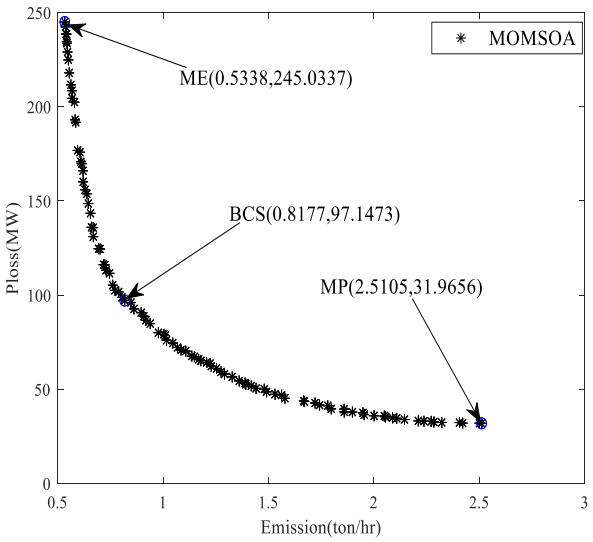

Fig. 20 The Pareto front of MOMSOA for Case 8

solutions, whose specific definition is shown in equation (29-31). A detailed description about *SP* is provided in the literature [49].

$$SP = \sqrt{\frac{1}{N-1}\sum_{i=1}^{N}\left(\bar{j} - j_i\right)^2} \tag{29}$$

$$j_i = \min_{k=1,2,\cdots N}\left(\sum_{l=1}^{M}\left|g_l^i - g_l^k\right|\right) \tag{30}$$

$$\bar{j} = \frac{1}{N}\sum_{k}^{N} j_k \tag{31}$$

The *SP* represents the distribution for POS, and a smaller *SP* value corresponds to a more uniformly distributed Pareto front. When *SP* is equal to 0, it means that all solutions have the same interval, in which case the distribution is the most uniform.

2) HV

The *HV* metric is employed to measure the volume of an objective space that is dominated by at least one solution from non-dominated solution set. *HV* provides a splendid indicator of the convergence and diversity of POS set. Contrary to the *SP* indicator, a larger *HV* indicator symbolizes more excellent diversity and convergence. Besides, a larger value of *HV* metric means that the solution set is closer to the true Pareto front. The specific definition of *HV* is shown in equation (32). The details of this indicator are explained in the literature [50].

$$HV = V\left(\bigcup_{i=1}^{S} v_i\right) \tag{32}$$

where v_i denotes the super volume formed by the reference point and the *i*th solution in the solution set.

3) Indicator Statistics

The average running time is employed to measure the solution speed of algorithms, which reflects the efficiency in handling the EED problems. The average running time of several algorithms obtained through 30 experiments are provided in TABLE. XXI. The improvements added to the original algorithm lead to that the solution time of MOMSOA will inevitably be larger than MOSOA, however, it is lower than classical algorithms.

The box plot is a powerful tool for statistics and provides visual analysis, which is a statistical plot utilized to show dispersion, upper bound, lower bound, median and outliers of a set of data. TABLE. XIX lists the means and standard deviations of *SP* index computed by all algorithms for the eight cases, and Fig. 21 displays the box plots derived from all data. The mean and standard deviation of *SP* index from proposed MOMSOA in each case are the smallest despite the presence of outliers sometimes, which indicates that MOMSOA can obtain a more uniformly distributed solution set. MOMSOA proves to be indeed more superior in its ability to handle the EED problems.

The specific medians and standard deviations calculated with respect to the *HV* index are summarized in TABLE. XX. In addition, the box plots of *HV* indicators are offered in Fig. 22. The *HV* mean and standard deviation of MOMSOA are larger than those of the compared algorithms in all cases, which indicates that the convergence and diversity of the solution sets obtained by MOMSOA are significantly stronger than those of the several compared algorithms. The ability of MOMSOA to search for more and optimal solutions in space once again demonstrates the superior ability of MOMSOA in solving EED problems.

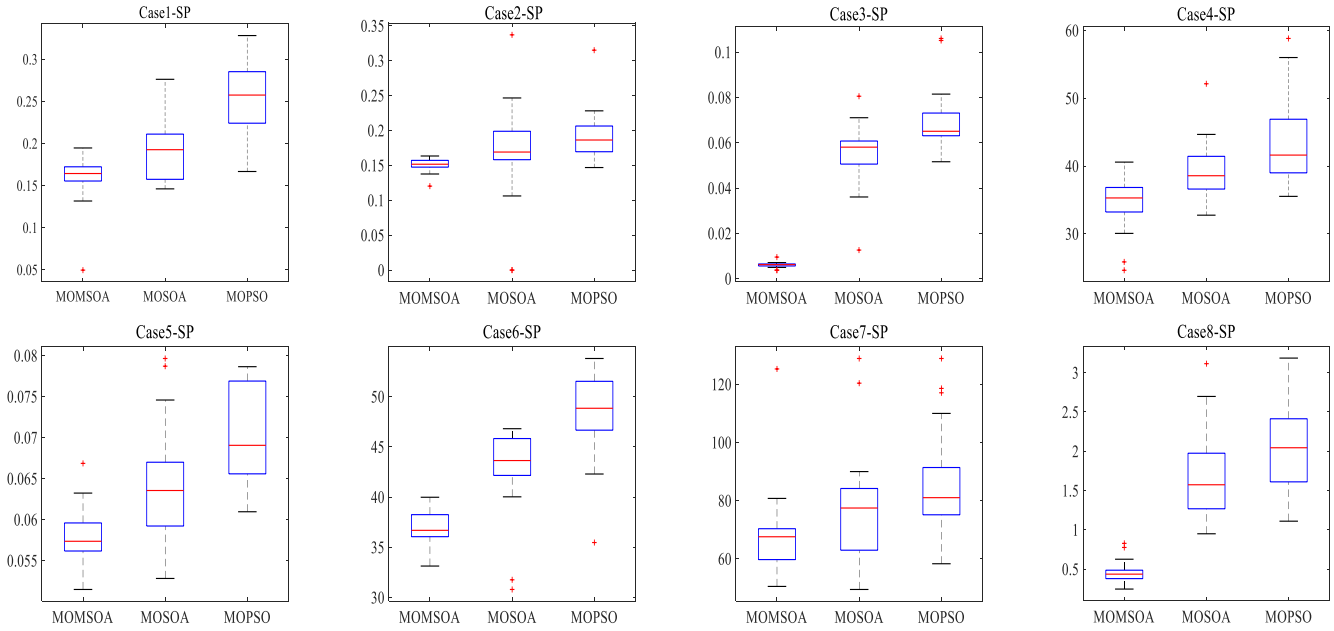

Fig. 21. *SP* indicators for eight cases

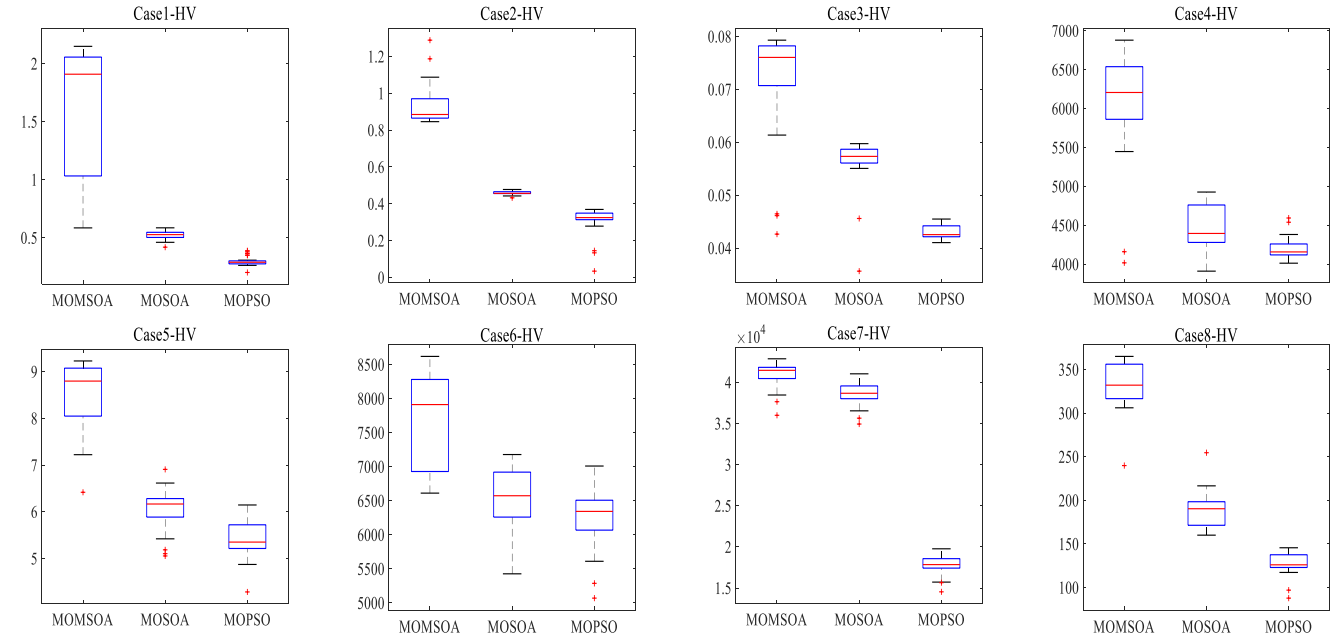

Fig. 22. *HV* indicators for eight cases

TABLE. XIX
MEAN AND STANDARD DEVIATION FROM DIFFERENT METHODS

Indicator	Cases	Data	Algorithms			
			MOMSOA	MOSOA	MOPSO	MODE
SP	1	mean	0.16008	0.19237	0.25544	-
		deviation	0.02488	0.03538	0.04114	-
	2	mean	0.15170	0.16778	0.19116	-
		deviation	0.00848	0.06315	0.03221	-
	3	mean	0.00606	0.05576	0.06963	-
		deviation	0.00101	0.01239	0.01222	-
	4	mean	34.6170	39.0210	43.4832	-
		deviation	3.51565	4.13075	5.61899	-
	5	mean	0.05805	0.06358	0.07085	-
		deviation	0.00328	0.00651	0.00644	-
	6	mean	36.8357	43.04334	48.3795	-
		deviation	1.690468	3.80365	3.92243	-
	7	mean	67.8006	76.7380	-	84.0046
		deviation	13.1256	17.3759	-	17.3592
	8	mean	0.44505	1.65412	-	2.03383
		deviation	0.12706	0.51378	-	0.53364

TABLE. XX
MEAN AND STANDARD DEVIATION FROM DIFFERENT METHODS

Indicator	Cases	Data	Algorithms			
			MOMSOA	MOSOA	MOPSO	MODE
HV	1	mean	1.60813	0.52359	0.29794	-
		deviation	0.58778	0.03824	0.04030	-
	2	mean	0.93184	0.45886	0.30743	-
		deviation	0.10173	0.00919	0.07418	-
	3	mean	0.07135	0.05653	0.04313	-
		deviation	0.01020	0.00475	0.00128	-
	4	mean	6075.08	4459.23	4205.19	-
		deviation	667.328	290.498	138.113	-
	5	mean	8.47024	6.04230	5.40987	-
		deviation	0.71169	0.42121	0.38136	-
	6	mean	7707.63	6542.56	6216.50	-
		deviation	631.245	444.669	451.402	-
	7	mean	41065.98	38652.21	-	17618.41
		deviation	1454.18	1360.77	-	1155.05
	8	mean	333.161	187.979	-	127.707
		deviation	26.1118	20.2117	-	13.1458

TABLE. XXI
RUNNING TIME OF ALL CASES

Algorithms	Cases							
	1	2	3	4	5	6	7	8
MOMSOA	125.67	124.02	126.28	223.96	229.03	238.96	1078.27	1102.29
MOSOA	133.08	128.58	130.84	230.39	237.76	242.85	1187.53	1146.01
MOPSO	153.75	148.76	136.48	226.06	246.89	240.73	-	-
MODE	-	-	-	-	-	-	1203.65	1182.83

V. CONCLUSION

In order to achieve economical and environmental operation in power systems, this paper proposes an improved search algorithm—MOMSOA, which combines logistic map, mutation operator and non-linear variation parameter *A*. Logistic map is innovatively utilized in the parameter optimization of this algorithm to effectively jump out of the local optimum. The exploration and exploitation of the algorithm are balanced by the cosine dynamic variation strategy which makes *A* non-linear. Combined with the mutation operator, the search process can cover a broader area to seek the global optimal solution more efficiently. What's more, a novel constraint handling strategy that combines non-inferior sorting is proposed to guarantee zero violation of constraints and to seek better PFs. To demonstrate the superiority of MOMSOA, comparative experiments of MOMSOA, MOSOA, and MOPSO/MODE were conducted on IEEE30-Bus, IEE57-Bus as well as IEEE118-Bus systems. In the meanwhile, the experimental results were also compared with the published literature. It turns out that MOMSOA can always obtains the optimal BCS and superior PF. In order to evaluate MOMSOA more comprehensively, performance metrics including *SP* and *HV* are calculated with all the experimental data. The results demonstrate that PFs obtained by MOMSOA have broader diversity and better convergence than MOSOA as well as MOPSO/MODE. Consequently, the proposed MOMSOA provides an efficient approach to deal with complex EED problems.

REFERENCES

[1] G. Chen, H. Zhuo, X. Hu, F. Long, and H. Long, "Environment Economic Power Dispatch from Power System Based on Multi-objective Novel Tree Seed Optimization Algorithm," *IAENG International Journal of Computer Science*, vol. 48, no. 4, pp. 845-861, 2021.

[2] G. Chen, X. Man, Y. Long, and Z. Zhang, "Application of Multi-objective New Whale Optimization Algorithm for Environment Economic Power Dispatch Problem," *Engineering Letters*, vol. 29, no. 1, pp. 68-81, 2021.

[3] L. Zhang, M. Khishe, M. Mohammadi, and A. H. Mohammed, "Environmental economic dispatch optimization using niching penalized chimp algorithm," *Energy*, vol. 261, article. 125259, 2022.

[4] L. Fu, H. Ouyang, C. Zhang, S. Li, and A. W. Mohamed, "A constrained cooperative adaptive multi-population differential evolutionary algorithm for economic load dispatch problems," *Applied Soft Computing*, vol. 121, article. 108719, 2022.

[5] S. Basak, B. Bhattacharyya and B. Dey, "Dynamic economic dispatch using hybrid CSAJAYA algorithm considering ramp rates and diverse wind profiles," *Intelligent Systems with Applications*, vol. 16, article. 200116, 2022.

[6] M. Afroozeh, H. R. Abdolmohammadi and M. E. Nazari, "Economic-environmental dispatch of integrated thermal-CHP-heat only system with temperature drop of the heat pipeline using mutant gray wolf optimization algorithm," *Electric Power Systems Research*, vol. 212, article. 108227, 2022.

[7] M. T. Hagh, S. M. S. Kalajahi and N. Ghorbani, "Solution to economic emission dispatch problem including wind farms using Exchange Market Algorithm Method," *Applied Soft Computing*, vol. 88, article. 106044, 2020.

[8] H. Nourianfar and H. Abdi, "Solving the multi-objective economic emission dispatch problems using Fast Non-Dominated Sorting TVAC-PSO combined with EMA," *Applied Soft Computing*, vol. 85, article. 105770, 2019.

[9] A. Carrillo-Galvez, F. Flores-Bazán and E. L. Parra, "Effect of models uncertainties on the emission constrained economic dispatch. A prediction interval-based approach," *Applied Energy*, vol. 317, article. 119070, 2022.

[10] L. Li, J. Lou, M. Tseng, M. K. Lim, and R. R. Tan, "A hybrid dynamic economic environmental dispatch model for balancing operating costs and pollutant emissions in renewable energy: A novel improved mayfly algorithm," *Expert Systems with Applications*, vol. 203, article. 117411, 2022.

[11] R. Zhang, K. Yan, G. Li, T. Jiang, X. Li, and H. Chen, "Privacy-preserving decentralized power system economic dispatch considering carbon capture power plants and carbon emission trading scheme via over-relaxed ADMM," *International Journal of Electrical Power & Energy Systems*, vol. 121, article. 106094, 2020.

[12] Z. Liu, L. Li, Y. Liu, J. Liu, H. Li, and Q. Shen, "Dynamic economic emission dispatch considering renewable energy generation: A novel multi-objective optimization approach," *Energy*, vol. 235, article. 121407, 2021.

[13] X. Chen and G. Tang, "Solving static and dynamic multi-area

economic dispatch problems using an improved competitive swarm optimization algorithm," *Energy*, vol. 238, article. 122035, 2022.
[14] L. Zhu, H. Ren, M. Habibi, K. J. Mohammed, and M. A. Khadimallah, "Predicting the environmental economic dispatch problem for reducing waste nonrenewable materials via an innovative constraint multi-objective Chimp Optimization Algorithm," *Journal of Cleaner Production*, vol. 365, article. 132697, 2022.
[15] V. K. Jadoun, G. R. Prashanth, S. S. Joshi, K. Narayanan, H. Malik, and F. P. G. Márquez, "Optimal fuzzy based economic emission dispatch of combined heat and power units using dynamically controlled Whale Optimization Algorithm," *Applied Energy*, vol. 315, article. 119033, 2022.
[16] H. Nourianfar and H. Abdi, "Solving the multi-objective economic emission dispatch problems using Fast Non-Dominated Sorting TVAC-PSO combined with EMA," *Applied Soft Computing*, vol. 85, article. 105770, 2019.
[17] A. Sundaram, "Multiobjective multi verse optimization algorithm to solve dynamic economic emission dispatch problem with transmission loss prediction by an artificial neural network," *Applied Soft Computing*, vol. 124, article. 109021, 2022.
[18] V. P. Sakthivel, M. Suman and P. D. Sathya, "Combined economic and emission power dispatch problems through multi-objective squirrel search algorithm," *Applied Soft Computing*, vol. 100, article. 106950, 2021.
[19] M. H. Hassan, D. Yousri, S. Kamel, and C. Rahmann, "A modified Marine predators algorithm for solving single- and multi-objective combined economic emission dispatch problems," *Computers & Industrial Engineering*, vol. 164, article. 107906, 2022.
[20] W. Hao, J. Wang, X. Li, H. Song, and Y. Bao, "Probability distribution arithmetic optimization algorithm based on variable order penalty functions to solve combined economic emission dispatch problem," *Applied Energy*, vol. 316, article. 119061, 2022.
[21] T. C. Bora, V. C. Mariani and L. D. S. Coelho, "Multi-objective optimization of the environmental-economic dispatch with reinforcement learning based on non-dominated sorting genetic algorithm," *Applied Thermal Engineering*, vol. 146, pp. 688-700, 2019.
[22] G. Dhiman and V. Kumar, "Seagull optimization algorithm: Theory and its applications for large-scale industrial engineering problems," *Knowledge-Based Systems*, vol. 165, pp. 169-196, 2019.
[23] G. Lei, H. Song and D. Rodriguez, "Power generation cost minimization of the grid-connected hybrid renewable energy system through optimal sizing using the modified seagull optimization technique," *Energy Reports*, vol. 6, pp. 3365-3376, 2020.
[24] L. Li, S. Zheng, M. Tseng, and Y. Liu, "Performance assessment of combined cooling, heating and power system operation strategy based on multi-objective seagull optimization algorithm," *Energy Conversion and Management*, vol. 244, article. 114443, 2021.
[25] Y. Wu, X. Sun, Y. Zhang, X. Zhong, and L. Cheng, "A Power Transformer Fault Diagnosis Method-Based Hybrid Improved Seagull Optimization Algorithm and Support Vector Machine," *IEEE Access*, vol. 10, pp. 17268-17286, 2022.
[26] M. Abdelhamid, E. H. Houssein, M. A. Mahdy, A. Selim, and S. Kamel, "An improved seagull optimization algorithm for optimal coordination of distance and directional over-current relays," *Expert Systems with Applications*, vol. 200, article. 116931, 2022.
[27] M. Ehteram, F. B. Banadkooki, C. M. Fai, M. Moslemzadeh, M. Sapitang, A. N. Ahmed, D. Irwan, and A. El-Shafie, "Optimal operation of multi-reservoir systems for increasing power generation using a seagull optimization algorithm and heading policy," *Energy Reports*, vol. 7, pp. 3703-3725, 2021.
[28] G. Dhiman, K. K. Singh, M. Soni, A. Nagar, M. Dehghani, A. Slowik, A. Kaur, A. Sharma, E. H. Houssein, and K. Cengiz, "MOSOA: A new multi-objective seagull optimization algorithm," *Expert Systems with Applications*, vol. 167, article. 114150, 2021.
[29] G. Chen, J. Qian, Z. Zhang, and S. Li, "Application of modified pigeon-inspired optimization algorithm and constraint-objective sorting rule on multi-objective optimal power flow problem," *Applied Soft Computing*, vol. 92, article. 106321, 2020.
[30] G. Chen, Q. Qin, Z. Ping, K. Peng, X. Zeng, H. Long, and M. Zou, "A Novel Approach Based on Modified and Hybrid Flower Pollination Algorithm to Solve Multi-objective Optimal Power Flow," *IAENG International Journal of Applied Mathematics*, vol. 51, no. 4, pp. 966-983, 2021.
[31] G. Chen, X. Yi, Z. Zhang, and H. Wang, "Applications of multi-objective dimension-based firefly algorithm to optimize the power losses, emission, and cost in power systems," *Applied Soft Computing*, vol. 68, pp. 322-342, 2018.
[32] H. T. Kahraman, M. Akbel and S. Duman, "Optimization of Optimal Power Flow Problem Using Multi-Objective Manta Ray Foraging Optimizer," *Applied Soft Computing*, vol. 116, article. 108334, 2022.
[33] B. Qiao, J. Liu and X. Hao, "A multi-objective differential evolution algorithm and a constraint handling mechanism based on variables proportion for dynamic economic emission dispatch problems," *Applied Soft Computing*, vol. 108, article. 107419, 2021.
[34] A. Sundaram, "Multiobjective multi verse optimization algorithm to solve dynamic economic emission dispatch problem with transmission loss prediction by an artificial neural network," *Applied Soft Computing*, vol. 124, article. 109021, 2022.
[35] M. Kohli and S. Arora, "Chaotic grey wolf optimization algorithm for constrained optimization problems," *Journal of Computational Design and Engineering*, vol. 5, no. 4, pp. 458-472, 2018.
[36] K. Deb, A. Pratap, S. Agarwal, and T. Meyarivan, "A fast and elitist multiobjective genetic algorithm: NSGA-II," *IEEE Transactions on Evolutionary Computation*, vol. 6, no. 2, pp. 182-197, 2002.
[37] G. Chen, J. Qian, Z. Zhang, and Z. Sun, "Applications of Novel Hybrid Bat Algorithm with Constrained Pareto Fuzzy Dominant Rule on Multi-Objective Optimal Power Flow Problems," *IEEE Access*, vol. 7, pp. 52060-52084, 2019.
[38] A. Ghasemi, "A fuzzified multi objective Interactive Honey Bee Mating Optimization for Environmental/Economic Power Dispatch with valve point effect," *International Journal of Electrical Power & Energy Systems*, vol. 49, pp. 308-321, 2013.
[39] G. Chen, J. Qian, Z. Zhang, and Z. Sun, "Many-objective New Bat Algorithm and Constraint-Priority Non-inferior Sorting Strategy for Optimal Power Flow," *Engineering Letters*, vol. 27, no. 4, pp. 882-892, 2019.
[40] G. Chen, J. Qian, Z. Zhang, and Z. Sun, "Applications of Novel Hybrid Bat Algorithm with Constrained Pareto Fuzzy Dominant Rule on Multi-Objective Optimal Power Flow Problems," *IEEE Access*, vol. 7, pp. 52060-52084, 2019.
[41] X. Yuan, B. Zhang, P. Wang, J. Liang, Y. Yuan, Y. Huang, and X. Lei, "Multi-objective optimal power flow based on improved strength Pareto evolutionary algorithm," *Energy*, vol. 122, pp. 70-82, 2017.
[42] P. K. Hota, A. K. Barisal and R. Chakrabarti, "Economic emission load dispatch through fuzzy based bacterial foraging algorithm," *International Journal of Electrical Power & Energy Systems*, vol. 32, no. 7, pp. 794-803, 2010.
[43] M. A. Abido, "Multiobjective particle swarm optimization for environmental/economic dispatch problem," *Electric Power Systems Research*, vol. 79, no. 7, pp. 1105-1113, 2009.
[44] A. A. A. E. Ela, M. A. Abido and S. R. Spea, "Differential evolution algorithm for emission constrained economic power dispatch problem," *Electric Power Systems Research*, vol. 80, no. 10, pp. 1286-1292, 2010.
[45] R. T. F. A. King, H. C. S. Rughooputh and K. Deb, "Solving the multiobjective environmental/economic dispatch problem with prohibited operating zones using NSGA-II," *IEEE*, pp. 298-303, 2011.
[46] M. A. Abido, "A novel multiobjective evolutionary algorithm for environmental/economic power dispatch," *Electric Power Systems Research*, vol. 65, no. 1, pp. 71-81, 2003.
[47] B. K. Panigrahi, V. R. Pandi, and S. Das, "Multiobjective fuzzy dominance based bacterial foraging algorithm to solve economic emission dispatch problem," *Energy*, vol. 35, no. 12, pp. 4761-4770, 2010.
[48] S. Hemamalini and S. P. Simon, "Emission constrained economic dispatch with valve-point effect using particle swarm optimization," *IEEE Xplore*, vol 1, pp. 1-6, 2008.
[49] T. Ding, C. Li, F. Li, T. Chen, and R. Liu, "A bi-objective DC-optimal power flow model using linear relaxation-based second order cone programming and its Pareto Frontier," *International Journal of Electrical Power & Energy Systems*, vol. 88, pp. 13-20, 2017.
[50] J. Qian, P. Wang, C. Pu, and G. Chen, "Joint application of multi-object beetle antennae search algorithm and BAS-BP fuel cost forecast network on optimal active power dispatch problems," *Knowledge-Based Systems*, vol. 226, article. 107149, 2021.